Phage dUTPases control transfer of virulence genes by a proto-oncogenic G protein-like mechanism

María Ángeles Tormo-Más[1‡], Jorge Donderis[2‡], María García-Caballer[1,3‡], Aaron Alt[2], Ignacio Mir-Sanchis[1], Alberto Marina[2,4,*], José R Penadés[2,3,*]

[1]Centro de Investigación y Tecnología Animal, Instituto Valenciano de Investigaciones Agrarias (CITA-IVIA), Apdo. 187, 12.400 Segorbe, Castellón, Spain,

[2]Instituto de Biomedicina de Valencia, Consejo Superior de Investigaciones Científicas (IBV-CSIC) 46010 Valencia, Spain,

[3]Departamento de Ciencias Biomédicas, Universidad Cardenal Herrera-CEU, 46113 Moncada, Valencia, Spain,

[4]Centro de Investigación Biomédica en Red de Enfermedades Raras (CIBERER).

Running title: Structural basis for dUTPase protein signalling

Keywords: *Staphylococcus aureus*, phage, pathogenicity island, SaPI induction, gene transfer, moonlighting proteins, dUTPase, dUTP, G protein, P-loop

*Corresponding authors:

José R. Penadés

Alberto Marina

Instituto de Biomedicina de Valencia, 46010 Valencia, Spain

Phone: +34 96339 17 54

Fax: +34 969 08 00

e-mails: jpenades@ibv.csic.es

amarina@ibv.csic.es

‡These authors contributed equally to this work.

SUMMARY

dUTPases (Duts) have emerged as promising regulatory molecules controlling relevant cellular processes. However, the mechanism underlying this regulatory function remains enigmatic. Using staphylococcal pathogenicity island (SaPI) repression as a model, we report here that phage Duts induce the transfer of SaPI-encoded virulence factors by switching between active (dUTP-bound) and inactive (apo state) conformations, a conversion catalysed by their intrinsic dUTPase activity. Crystallographic and mutagenic analyses demonstrate that binding to dUTP re-orders the C-terminal motif V of the phage-encoded Duts, rendering these proteins into the active conformation required for SaPI derepression. By contrast, the conversion to the apo state conformation by hydrolysis of the bound dUTP generates a protein that is unable to induce the SaPI cycle. Because none of the requirements involving Duts in SaPI transfer is exclusive to the phage-encoded proteins, we propose that Duts are widespread cellular regulators acting in an analogous manner to the eukaryotic G proteins.

INTRODUCTION

Preserving DNA integrity is of vital importance for all organisms. Cellular metabolism constantly generates non-canonical nucleoside triphosphates, such as dUTP, dITP, dXTP, 8-oxo-dGTP or 2-oxo-dATP, which arise from oxidation, deamination or from other modifications of canonical nucleotides. Incorporation of non-canonical nucleotides into the nascent DNA results in increased mutagenesis and overloads the DNA excision repair system, leading to multiple DNA strand breaks and cell death. The most common non-canonical nucleoside triphosphate is dUTP, which is continuously produced in the pyrimidine biosynthesis pathway by phosphorylation of dUDP or by deamination of dCTP (Vértessy and Tóth, 2009). Most DNA polymerases cannot distinguish between thymine and uracil (except for some archaeal enzymes), and the uracil/thymine incorporation ratio depends on the relative level of dUTP and dTTP. Genomes of all free-living organisms and many viruses encode the enzyme dUTPase (dUTP pyrophosphatase; Dut; EC 3.6.1.23), which cleaves dUTP into dUMP and pyrophosphate and plays a key role in preventing uracil misincorporation into DNA (Vértessy and Tóth, 2009). It has been traditionally assumed that Duts are essential for DNA integrity and viability in many prokaryotic and eukaryotic organisms including *Escherichia coli, Saccharomyces cerevisiae,* trypanosomes and human cancer cells (Koehler and Ladner, 2004; Kouzminova and Kuzminov, 2004; Whittingham et al., 2005; Tchigvintsev et al., 2011), functions that are related with the role that the enzyme plays in preventing dUTP incorporation into the chromosome.

However, recent reports using completely different models have done away with the dogma that DNA uracilation is deleterious under all conditions. Deamination of cytosine bases in DNA to uracil by the activation-induced deaminase (AID) is essentially required for the diversity of immunoglobulin genes (Petersen-Mahrt et al., 2002; Maul et al., 2011). On the other hand, rather than being dangerous, HIV DNA uracilation benefits the early phase of the viral life cycle by inhibiting autointegration (Yan et al., 2011).

Finally, it has recently been demonstrated that *Drosophila melanogaster* tolerates high levels of uracil in DNA during some developmental stages, suggesting a novel role of uracil-containing DNA in *Drosophila* metamorphosis (Muha et al., 2012). If we assume that DNA uracilation is beneficial in some biological processes, and since the cellular enzyme Dut is present in these scenarios, it is tempting to speculate that these enzymes perform additional functions in the cell.

Most viruses, including herpes viruses, poxviruses, retroviruses and bacteriophages, encode Dut. It is an intriguing question, however, why these viruses encode an enzyme that is already present in all of their eukaryotic or prokaryotic host cells. Recent studies support the hypothesis that virus-encoded Duts could be moonlighting as proteins with different regulatory functions. Thus, the Epstein-Barr virus (EBV) Dut activates NF-κB expression and produces immune dysregulation in the host by binding to the cellular Toll-like receptor 2 (Glaser et al., 2006; Ariza et al., 2009). This same receptor is the target for the human endogenous retrovirus K (HERV-K) Dut, which has recently been found to be involved as a potential contributor to psoriasis pathophysiology (Ariza and Williams, 2011). In the same manner, Leang and coworkers demonstrated that the expression of the MHV-68 viral Dut is essential in this viral infective process by blocking the expression of the type I interferon signalling pathway, a process that does not depend on the intrinsic enzymatic activity of MHV-68 viral Dut (Leang et al., 2011). Finally, its has recently reported that the Kaposi's sarcoma Dut down-regulates the immune response by targeting several cytokine receptors, a process that does not depend of the enzymatic activity of the protein (Madrid and Ganem, 2012).

In a previous work, we also demonstrated that Duts have regulatory functions that involve the proteins in the control of the transfer of different *Staphylococcus aureus* pathogenicity islands (SaPIs) (Tormo-Más et al., 2010). SaPIs are a family of related 15–17 kb mobile genetic elements that carry and disseminate superantigen and other virulence genes, especially those for toxic shock toxin and enterotoxin B (Novick et al.,

2010). SaPIs are very widespread among the staphylococci and are responsible for at least one important human disease: menstrual toxic shock syndrome. The key feature of their mobility and spread is the induction by certain phages of their excision, replication and efficient encapsidation into specific small-headed phage-like infectious particles. This sequence of events is referred to as the SaPI excision–replication–packaging (ERP) cycle (reviewed in Novick et al., 2010). In the absence of a helper phage, the SaPIs reside passively in the host chromosome, under the control of Stl, a global SaPI-coded repressor (Úbeda et al., 2008). Following infection by a helper phage, the SaPI cycle is induced, and the SaPIs are finally packaged in phage-like particles composed of phage virion proteins, leading to very high frequencies of inter- as well as intrageneric transfers (Chen and Novick, 2009; Maiques et al., 2007). Surprisingly, the de-repressor protein for a subset of clinically relevant pathogenicity islands (including the prototype SaPIbov1, SaPIbov5, SaPIov1 and SaPIS0385) are helper phage-encoded Duts, which bind to the SaPI-encoded repressor Stl and act as antirepressors (Tormo-Más et al., 2010). However, how Dut proteins interact with the SaPI-encoded Stl repressor, and how this interaction leads to SaPI derepression remains to be elucidated.

In this manuscript we report that phage-encoded Duts control the transfer of SaPIs by an entirely novel and surprising strategy wherein these proteins are involved in cellular signalling. Namely, we have demonstrated that in addition to the 5 classical domains present in all trimeric Duts, staphylococcal phage-encoded Dut proteins have an extra region (domain VI) involved in SaPI de-repression by binding to the SaPI-encoded repressor (Stl). This extra domain, although necessary, is not sufficient to induce the SaPI cycle. In addition, Duts control the transfer of SaPIs by switching between the active (dUTP-bound) and inactive (apo state) conformations, a conversion catalysed by their intrinsic dUTPase activity. As reported for the proto-oncogenic G proteins, we propose that Dut proteins have an active dUTP-bound state that interacts with their specific targets. The hydrolysis of the bound dUTP by their intrinsic dUTPase activity triggers a

123 conformational change to a more relaxed conformation that releases the target protein
124 and downregulates the inducing activity by returning the Dut proteins to their resting state.
125 In addition, and as previously suggested for dUTP (Williams et al., 2011) and reported for
126 other nucleotides, our results support an emerging role for dUTP as second messenger.

127

128 **RESULTS**

129 **SaPI induction depends on Dut conformation**

130 In a previous work, we demonstrated that the expression of the cloned phage ϕ11 Dut
131 protein induced the SaPIbov1 cycle (Tormo-Más et al., 2010). Moreover, we also
132 demonstrated that the expression of the inactive mutant phage ϕ11 D81A Dut was also
133 capable of inducing SaPIbov1, indicating that dUTPase activity *per se* is not responsible
134 for SaPI induction (Tormo-Más et al., 2010). However, a more exhaustive analysis have
135 now revealed that the wild-type and D81A forms of the cloned phage ϕ11 or ϕ71 Duts
136 exhibited the same SaPIbov1 derepression activity only when they were fully over-
137 expressed, but reduced expressions of dut^{D81A} failed to derepress SaPIbov1, although
138 there was still full derepression by dut^{wt} under these conditions (Figure 1). A more
139 dramatic example of this behaviour was seen in a complementation analysis using the
140 phage 80α D81A mutant Dut, which was unable to induce SaPIbov1 even when
141 expressed at a high level (Figure 1). This result was confirmed *in vivo* by generating a
142 lysogenic strain for the 80α phage carrying the Dut D81A mutation in the phage genome.
143 As expected, the phage expressing the D81A mutant protein did not induce SaPIbov1
144 (Figure 2). Similar results were obtained with SaPIbov5, which is also induced by the
145 Dut80α protein (Figure 2). As the Dut protein levels produced from the wild-type (wt) and
146 D81A mutant were comparable in all these experiments (Figures 1 and 2), we concluded
147 that the wt Dut proteins are more effective than the D81A mutants in the de-repression of
148 SaPIbov1 and SaPIbov5.

What are the structural bases for this difference? The previous results raised a surprising possibility of Dut-Stl interaction that we decided to explore; namely, that the Dut proteins had two conformations with different inducing capacities. The SaPI-inducing conformation would correspond to that adopted by the wild-type Dut proteins, whereas the non-inducing conformation would be adopted by the D81A mutants.

The dUTP-bound form of the phage 80α-encoded Dut induces the SaPI cycle

In all the trimeric Dut proteins, the equivalent position of D81 is strictly occupied by a conserved catalytic aspartic residue (Barabas, 2004). This acidic residue localises and polarises a water molecule for an in-line nucleophilic attack on the αP during dUTP hydrolysis (Barabas, 2004; Chan et al., 2004). The conservative mutation D $\rightarrow$ N of the equivalent residue in the human Dut impairs the water molecule accommodation, rendering enzymes with nearly null catalytic activity, but also generally preserves dUTP-binding capacity (Barabas, 2004). In addition, this mutant is predicted to have disordered the C-terminal region of the trimeric proteins (named motif V), as adequate interaction among the D81 residue, the catalytic water and the substrate dUTP are required for the correct ordering of this domain in the human Dut (Varga et al., 2007).

In agreement with previous results concerning the human Dut protein (Barabas, 2004), calorimetric studies using purified Dut80α^{wt}, Dut80α^{D81A} and Dut80α^{D81N} proteins confirmed that the D81 mutants presented only a slightly reduced dUTP-binding capacity (3-fold reduction, Figure S1, Table S1) but an extremely low hydrolytic activity (not detectable in our enzymatic assay) when compared with the wild-type Dut80α (Table S1). In addition, and as expected given the mutation affected the same catalytic D81 residue, the Dut80α^{D81N} mutant was unable to induce SaPIbov1 or SaPIbov5 (Figure 2).

In light of these results, we hypothesised that the different inducing capacities observed in the Dut80α^{wt} and D81 mutants were related to conformational changes induced during the proper nucleotide binding process. To confirm this hypothesis, the

175 structures of both the Dut80α^{wt} apoenzyme and its ternary complexes with the non-
176 hydrolysable dUTP analogue α,β-imido-dUTP (dUMpNpp) with Mg^{2+} were determined at
177 2.9 Å and 2.8 Å resolution, respectively (Table 1). Note that these two forms correspond
178 to those present *in vivo*, as once Duts hydrolyse dUTP to yield dUMP and PPi, dUMP
179 dissociates quickly from the active centre (Vértessy and Tóth, 2009).

180 Dut80α^{wt} presents a prototypical homotrimeric Duts organization with three
181 independent active sites, each of which is formed by five conserved motifs (Figures 3-4
182 and S2). All three subunits contribute to each active site: motifs I, II and IV from one
183 subunit contribute to the binding of the triphosphate moiety, motif III from the adjacent
184 protomer is involved in nucleoside binding and provides the catalytic aspartate (D81 in
185 Dut80α), while the aforementioned motif V from the third subunit is the swapping P-loop-
186 like element covering the dUTP triphosphate (Figures 3-4 and S2).

187 Interestingly, Dut80α^{wt} contains an additional motif VI (residues 99-124; Figures 3-
188 4 and S2) that corresponds to a divergent region present in many uncharacterized phage-
189 encoded Duts (Tormo-Más et al., 2010) but absent from the structurally-related human-
190 encoded Dut protein (Figure S3). This extension folds as an L-shape β-hairpin, which,
191 being laterally projected from the rim of a characteristic channel formed at the trimer
192 interface, rests in the molecule main body (Figures 3-4 and S2-S3). As our previous
193 studies demonstrated that this extra domain modulates the affinity of the different phage-
194 encoded Dut proteins for the SaPIbov1 repressor Stl (Tormo-Más et al., 2010), we
195 hypothesised that the nucleotide-regulated Dut-Stl recognition mechanism could be
196 mediated by alternative conformations of this extension depending on the presence of
197 dUTP. This was not the case. Superimposition of the apo- and nucleotide-bound
198 structures revealed that the conformation of this extra motif remained constant (Figures 3-
199 4, S2 and S4). Indeed both structures were basically indistinguishable (rmsd of 0.58 Å for
200 154 residues; Table S2), except for motif V, which was not visible in the apoenzyme
201 (Figure 3-4 and S2). This observation agrees with previous structural data, including that

of prokaryotic and eukaryotic dUTPases, which demonstrated that dUTP binding induces a major conformational change restricted to motif V (Vertessy et al., 1998), the proper organisation of which is essential for catalysis (Varga et al., 2007; Freeman et al., 2009; Pécsi et al., 2011). Motif V caps the active site upon ligand binding and is necessary for efficient substrate discrimination and dUTP hydrolysis but not for nucleotide binding or structural integrity (Vertessy, 1997; Freeman et al., 2009; Pécsi et al., 2011). Interactions of Dut80α motif V residues with the dUMpNpp phosphates, sugar and base confirm the role of this structural element in nucleotide discrimination and binding (Figure 3D and 3E). In addition, the conserved motif V R160 residue, which is essential for dUTP hydrolysis (Pécsi et al, 2012), participates actively in the contact network required to localize and to activate the nucleophilic water by forming a salt-bridge with the catalytic Asp (Figure 3E). This network also includes hydrogen bonds of this nucleophilic water with the conserved Q137 and with the main chain of K79 (Figure 3E). Likewise in Dut80α, motif V is disordered in various Dut structures and is ordered only in the presence of the non-hydrolysable analogues of dUTP (Varga et al., 2007), suggesting that the dUTP-induced motif V organisation could be responsible for the conformational switch that triggers Dut-Stl binding.

If our hypothesis was correct, the 3D structure of the Dut80α^{D81A} and Dut80α^{D81N} mutants should be identical to that observed in the apo state of the Dut80α^{wt} protein. To test this, we solved the X-ray structures of the Dut80α^{D81A} and Dut80α^{D81N} mutants (2.9 and 3.0 Å resolution, respectively; Table 1). As predicted, the 3D structures of both D81 mutants in the presence of the dUMpNpp were practically identical to that of the wild-type apoenzyme (Figures 4-5, S2, and S4-S5; Table S2). Matching results were obtained with the 3D structures of the D81 mutants in the absence of dUMpNpp (data not shown). Like the wild-type apoenzyme, motif V was totally disordered in both mutants even though the active centre was occupied by the nucleotide in the Dut80α^{D81A} and Dut80α^{D81N} structures (Figures 4-5, S2 and S5). This result confirmed that the proper location of the nucleophilic

water molecule by the catalytic aspartic (D81) residue is essential for motif V organisation (Varga et al., 2007), and the result supports the notion that the catalytically-competent disposition of motif V is a key element for interaction with Stl. In agreement with this notion, the expression of Dut80α-mutant protein carrying a deletion in motif V (ΔV) was unable to induce SaPIbov1 and SaPIbov5 replication (Figure 2).

To clearly confirm that the binding of the nucleotides induced the conformational changes that control SaPIbov1 induction, three additional mutants (Y84F, Y84A and Y84I) of the strictly conserved Tyr (Y84), responsible for deoxyribose discrimination, were structurally and functionally analysed (Figure 2; Table1). The Y84I mutant presented a null dUTP-binding capacity (Figure S1, Table S1) and was unable to order the C-terminal motif V of the protein (Figures 4, S2 and S5). Consequently, Dut80α^{Y84I} neither induced SaPIbov1 nor SaPIbov5 (Figure 2). The structure, basically identical to that observed in the apo state, indicates that dUMpNpp is not bound to the active centre that is partially occupied by the new Ile side-chain (Figures 4, S2, S4-5; Table S2). By contrast, Dut80α^{Y84F} presented almost wild-type dUTP-binding capacity and activity (Figure S1, Table S1), induced the SaPI cycle (Figure 2) and had a P-loop motif V that was well ordered over the nucleotide (Figures 4-5, S2 and S4; Table S2). Interestingly, intermediate properties were observed for the Y84A mutant. This mutant presented a reduced dUTP-binding capacity but retained some enzymatic activity (Figure S1, Table S1). These findings correlate well with an increased conformational freedom for the C-terminal motif V, which was reflected in the poor local electron density that only enabled us to build a partial model for this region (Figures 4, S2, S4-5 and S6). As expected, expression of the Dut80α^{Y84A} protein did not induce the SaPIbov1 cycle (Figure 2). As previously demonstrated, the Dut-Stl interaction requires a stable motif V in the catalytically-competent conformation.

The proper conformation of the Dut P-loop motif V, but not the dUTPase activity, is required for SaPI induction

In a previous work we proposed that the dUTPase activity was not required to derepress the SaPI cycle (Tormo-Más et al., 2010). This was supported by the analysis of the Dut80α^{D95E} mutant, which retained the enzymatic activity but did not induce SaPIbov1. In addition, overexpression of the inactive ϕ11 Dut^{D81A} protein from plasmid pCN51 induced SaPIbov1 (Figure 1)(Tormo-Más et al., 2010). However, the data reported herein appears to contradict this confirmation, as only those proteins with a wild-type enzymatic activity induced SaPIbov1. Based on our crystallographic data, and to clearly confirm that the unique role for the enzymatic activity in derepressing SaPIbov1 is to properly order and stabilise the C-terminal motif V, we introduced into the enzymatically inactive Dut80α^{D81A} mutant substitutions in the D110 (motif VI) and S168 (motif V) residues, converting these residues to cysteines (D110C and S168C). The proximity of these residues (Figure 3) is predicted to allow disulphide bond formation, rendering motif V competent for SaPI derepression. To confirm that the proposed intersubunit disulphide bound was indeed formed and motif V was ordered, we solved the crystal structure of Dut80$\alpha^{D81A\text{-}CC}$ mutant (2.6 Å resolution; Table 1). The disulphide bound linking C110 and C168 was easily modelled following the density map as well as the motif V that presented a quite similar wild-type conformation (Figures 4-5 and S2), except for the last three residues (Figure S4B). dUMP but not dUMpNpp was present in the Dut80$\alpha^{D81A\text{-}CC}$ active center, even though 5 mM dUMpNpp was added to the crystallization cocktail. This nucleotide was co-purified with the protein, suggesting that the restricted mobility of the motif V imposed by the disulphide bound limited the nucleotide dissociation. As proposed, these changes generated a mutant protein (Dut80$\alpha^{D81A\text{-}CC}$) without enzymatic activity (Table S1) but with a greater capacity to induce SaPIbov1 replication than the wt Dut80α protein (Figure 2), suggesting that the limited differences observed in the motif V conformation (Figure S4B) have a minor impact on Stl binding, or that the Stl repressor induces a motif V fit during the binding process. Interestingly, the increased capacity of this mutant to induce the SaPI cycle can be explained because this protein does not exhibit an allosteric response to the

dUTP pool. Note, however, that this increased replication was not accompanied with an increased SaPI transfer (Figure 1), confirming that an extensive SaPI replication is not required for high-frequency SaPI transfer (Úbeda et al., 2008). A possible explanation for this is given below.

The Dut mutant proteins differ in their affinity for the SaPI-encoded Stl repressor

We have previously demonstrated that the only function for the phage-encoded Dut proteins in the SaPI cycle is to disrupt the binding of the SaPI-encoded Stl repressor to its target DNA site (Tormo-Más et al., 2010). Consequently, it was predicted that different Dut mutant proteins should induce transcription of the Stl-repressed SaPIbov1 genes in a different manner. This was confirmed using plasmid pJP674, which carries a β-lactamase reporter gene fused to *xis*, downstream of *str* and the Stl-repressed *str* promoter, and also encodes Stl (see Figure 6A). This plasmid was introduced into strains expressing the different cloned Dut proteins and expression was tested in the presence of an inducing concentration of $CdCl_2$. Induction of the plasmids expressing Dut80α^{wt}, Dut80α^{Y84F} or Dut80$\alpha^{D81A\text{-}CC}$ proteins increased β-lactamase expression, but plasmids lacking the motif V (ΔV) or carrying the D81A, D81N, Y84A or Y84I mutations did not induced β-lactamase expression (Figure 6A). As expected, the Dut80$\alpha^{D81A\text{-}CC}$ mutant protein demonstrated increased affinity for the Stl repressor compared with the wt and the Y84F Dut proteins (Figure 6A). These results confirm our previous results from the SaPI replication analysis (Figure 2). We conclude from these latest results that the conformational changes observed previously determine the binding capacities of the Dut proteins for the Stl repressor.

The switch on/off mechanism prevents uncontrolled SaPI replication

The process by which the staphylococcal pathogenicity islands have acquired the ability to exploit the dUTP-mediated conformational change of Duts as an antirepressor represents a remarkable evolutionary adaptation. Why is a strictly controlled mechanism needed to

induce SaPIbov1? We have previously reported that an inactivating mutation in any SaPI-encoded Stl repressor provokes an uncontrolled SaPI replication that does not increase SaPI transfer but severely affects bacterial viability (Úbeda et al., 2008). This was also observed after expression of the Dut80$\alpha^{D81A\text{-}CC}$ mutant protein, which did not increase SaPI transfer but severely affected bacterial growth (Figures 1 and 6B). Consequently, and as SaPIs require some cellular components to be efficiently transferred, it is logical that they make use of an on/off mechanism to prevent uncontrolled replication.

DISCUSSION

Our previous results have demonstrated that staphylococcal phage-encoded Duts control both the induction and transfer of SaPIs by a mechanism (see the scheme in Figure 7) similar to that reported for the proto-oncogenic G proteins. Mammalian G proteins are a large family of GTP-regulated molecular switches in signalling pathways that modulate many cell behaviour aspects, including proliferation, differentiation, motility and death (Etienne-Manneville and Hall, 2002). Normally, these proteins have an active GTP-bound state that interacts with the targets. The hydrolysis of the bound GTP by its intrinsic or induced GTPase activity triggers a conformational change to a more relaxed conformation of two γ-phosphate interacting switch regions, which, in turn, release the target protein and turn off their activity by returning G proteins to their resting state (Vetter and Wittinghofer, 2001). This mechanism is similar to that described herein for the SaPI-inducing capacities of the phage-encoded Duts, but in this case involving a single switch, the P-loop motif V. If we bear in mind the high motif V conservation, this element must be responsible for the on/off mechanism, with the characteristic additional motif (extra motif VI) present in these phage-encoded Duts providing the specificity for the target protein (Stl in the case of staphylococcal phage-encoded Dut proteins). We have previously reported that this extra domain controls the affinity between the Dut and the Stl proteins (Tormo-Más et al., 2010). However, although involved in the process, the domain is not sufficient

to induce the SaPI cycle, as demonstrated here. The connection between these two motifs is highlighted by their close proximity (e.g., the hydrophobic interaction of Ile109 with Val170 in the insertion and P-loop-like structural elements, respectively) observed in the Dutα80-dUMpNpp structure (Figure 3).

It has been previously reported that the rat Dut protein interacts with the transcriptional factor PPARα (peroxisome proliferator-activated receptor alpha), repressing the PPAR-mediated transcriptional activation (Chu et al., 1996). Analogously to the Stl-Dut interaction presented herein, the rat Dut-PPARα interaction depends on an "extra" N-terminal motif VI present in the rat Dut protein, and requires the C-terminal domain contribution (Chu et al., 1996), strongly suggesting as a general theme the current mechanism involving Duts in signalling. Do we have any extra evidence that supports the hypothesis that the mechanism described herein involving Duts in signalling is widespread? As expected for a general mechanism, none of the three requirements for the Dut-mediated signalling is exclusive to the staphylococcal phage-encoded Dut proteins. Firstly, it has been extensively reported that binding of dUTP orders motif V in all trimeric Duts tested (Vertessy et al., 1998; Varga et al., 2007; Freeman et al., 2009; Pécsi et al., 2011). Secondly, the existence of extra domains in the Dut proteins has been previously reported for the aforementioned rat, *Drosophila melanogaster*, *Plasmodium falciparum* and *Mycobacterium tuberculosis* Dut proteins (Chan et al., 2004; Dubrovay, 2004; Whittingham et al., 2005). In addition, a database search revealed the existence of multiple prokaryotic and eukaryotic dUTPases carrying extra domains (Figure S7). Although the roles of these extra domains have not yet been identified, recent studies have demonstrated that the deletion of the mycobacteria-specific loop, which is close to the C-terminal region, has no major effect on dUTPase enzymatic properties despite the region being essential in the living cell (Pécsi et al., 2012). Finally, Dut-mediated protein-protein interactions with specific partners have also been reported. For example, as mentioned previously, the EBV and HERV-K viral Duts interact with Toll-like receptor 2

(Ariza et al., 2009; Ariza and Williams, 2011), while the MHV-68 viral Dut blocks the type I interferon-dependent signalling pathway (Leang et al., 2011). In eukaryotes, in addition to the aforementioned Dut:PPARα interaction (Chu et al., 1996), recent interactomics studies have revealed several promising Dut partners that need further confirmation. For example, the implication of human Dut in processes such as apoptosis, autophagy, and controlling the epidermal growth factor signalling pathway (by interacting with the Rho-related GTP-binding protein RhoB, the associated GABA receptor proteins GABARAPL1, GABARAPL2 and GABARAP, the growth hormone 1 GH1 and the nuclear oestrogen receptor) has been suggested (Blagoev et al., 2003; Ewing et al., 2007; Kim et al., 2009; Behrends et al., 2010). Furthermore, yeast Dut interaction studies implicate several regulatory proteins, including the GTPase-interacting proteins TEM1, MUK1 and eIF-2B, along with the cyclin-dependent kinase CKS1 (Ito et al., 2001; Ho et al., 2002; Yu et al., 2008).

In summary, all these results strongly support the idea that the mechanism described herein for the Dut-Stl interaction is widespread. Although additional studies are necessary to define the signalling pathways activated by the these proteins and to determine how dUTP controls these processes, our results suggest that dUTPases define a new family of relevant signalling molecules involved in several relevant pathogenic processes.

EXPERIMENTAL PROCEDURES

Bacterial strains and growth conditions

The bacterial strains used in these studies are listed in Table S3. The procedures for preparation and analysis of phage lysates, in addition to transduction and transformation of *S. aureus,* were performed essentially as previously described (Tormo-Más et al., 2010).

DNA methods

General DNA manipulations were performed using standard procedures. The oligonucleotides used in this study are listed in Table S4. The labelling of the probes and DNA hybridization were performed according to the protocol supplied with the PCR-DIG DNA-labelling and Chemiluminescent Detection Kit (Roche).

To produce the *dut* mutations, we used plasmid pMAD, as previously described (Tormo-Más et al., 2010).

Plasmid construction

The plasmid constructs were prepared by cloning PCR products obtained with the oligonucleotide primers listed in Table S4. All clones were sequenced by the Institute Core Sequencing Lab. Dut proteins were expressed in *S. aureus* under inducing conditions from the P*cad* promoter in the expression vector pCN51, as previously described (Tormo-Más et al., 2010).

Enzyme assays

β-Lactamase assays, using nitrocefin as a substrate, were performed as described (Tormo-Más et al., 2010). β-Lactamase activities were recorded as initial slopes divided by cell density (Vmax)/OD_{650}.

dUTPase enzyme activity assays were performed using the EnzCheck Pyrophosphate Assay Kit (Molecular Probes).

Isothermal titration microcalorimetry (ITC)

ITC was used to evaluate the dissociation constants of Dut80α and mutants against dUMpNpp. All experiments were carried out at 25º C with protein concentrations between 20 and 30 mM and nucleotide concentrations between 150 mM and 400 mM in 25 mM Tris, pH 8.0. The reactions were performed in an AUTO ITC instrument Microcal Auto-iTC200. Data integration, correction and analysis were carried out using Origin 7 (Microcal) with a single-site binding model.

Production of wild-type and mutant proteins

His-tagged wt and mutant Dut proteins were produced in *E. coli* BL21 (DE3) (Novagen) strain transformed with the corresponding gene cloned in pET-28a plasmid (Novagen). Proteins were overexpressed in *E. coli* by first growing the cells at 37 ºC in LB medium supplemented with 33 µg/ml kanamycin to OD_{600}=0.5-0.6 and then inducing expression with 1 mM isopropyl-β-D thiogalactopyranoside (IPTG) for 3 h. Cells were collected by centrifugation and resuspended in buffer A (100 mM Tris pH 8.0, 150 mM NaCl) supplemented with 1 mM phenylmethanesulfonyl fluoride (PMSF). Cells were lysed by sonication and soluble proteins present in the supernatant were loaded on a His Trap HP column (GE Healthcare) equilibrated with buffer A. The resin was washed with buffer A supplemented with 10 mM imidazole and proteins were eluted with buffer A supplemented with 350 mM imidazole. Duts were concentrated and loaded onoto a Superdex S200 (GE Healthcare) equilibrated with buffer A. Fractions were analysed by SDS/PAGE and the purest fractions were pooled, concentrated and stored at -80 ºC.

Crystallization, data collection, and model building

The crystals were grown as hanging drops at 21ºC with a vapour-diffusion approach. Wild-type Dut80α and the mutant forms (6-9 mg/ml) in the presence of 5mM dUMpNpp and 10 mM $MgCl_2$ were crystallized from solutions of 2-6% *tert*-butanol $(NH_4)_2SO_4$, 0.1 M Tris (pH 8.5) and either 30-50% MPD or 30-50% PEG400. Apo Dut80α crystals were obtained in similar conditions but in the absence of nucleotide. Crystals were directly frozen in liquid N_2 and X-ray diffraction was carried out at 100 K at the ESRF and DLS synchrotrons or in home (Supernova X-ray microsource from Agilent). All the Dut80α crystals belonged to space group $P2_13$ and presented similar cell size with a monomer in the asymmetric unit (Table 1). The final model of apo Dut80α was obtained after iterative building and refining with Coot and CCP4 suite programs. The phases were obtained by molecular replacement using the structure of human Dut (PDB 2HQU) as a search model. Apo Dut80α structure was used as initial model for the refinement and model building of the rest of Dut structures (Table 1).

Accession numbers

Coordinates and structure factors have been deposited with the RCSB Protein Data Bank (http://www.rcsb.org/pdb/) under accession codes 3zez (wt Dut80α-dUMpNpp), 3zf2 (wt Dut80α-apo), 3zf0 (Dut80α D81A-dUMpNpp), 3zf1(Dut80α D81N-dUMpNpp), 3zf3 (Dut80α Y84I), 3zf4 (Dut80α Y84A-dUMpNpp), 3zf5 (Dut80α Y84F-dUMpNpp) and 3zf6 (Dut80α D81A C110 C168-dUMP).

ACKNOWLEDGMENTS

We thank Sonia Juan Rubio for her effort in making Figure 6 and Ramon Hurtado for his help in the ITC experiments. We also thank Richard P Novick, Beata Vertessy, Erwin Knecht, Íñigo Lasa, Ignacio Fita and Jean-Marc Ghigo for helpful comments on the manuscript. This work was supported by grants BIO2011-30503-C02-01 and Eranet-pathogenomics PIM2010EPA-00606 to J.R.P, and BIO2010-15424 to A.M., from the Ministerio de Ciencia e Innovación (MICINN), grants from the Cardenal Herrera-CEU University (Copernicus-Santander program) to J.R.P., and grants Consolider-Ingenio CSD2009-00006 and INIA-DR08-0093 to M.A.T-M..

Author Contributions

J.R.P. and A.M. conceived and designed the study; M.A.T.-M., M.G.-C. and I.M. characterized the mutants and performed gene expression experiments; J.D. and A.A. performed crystallographic analysis; J.R.P, A.M., M.A.T.-M., J.D., M.G.-C., A.A, and I.M analysed the data; J.R.P. and A.M. supervised the research; J.R.P and A.M. wrote the manuscript; J.R.P., A.M. and M.A.T-M. obtained funding.

REFERENCES

Ariza, M.-E., and Williams, M.V. (2011). A human endogenous retrovirus K dUTPase triggers a TH1, TH17 cytokine response: does It have a role in psoriasis? J. Investig. Dermatol. *131*, 2419–2427.

Ariza, M.-E., Glaser, R., Kaumaya, P.T.P., Jones, C., and Williams, M.V. (2009). The EBV-encoded dUTPase activates NF-kappa B through the TLR2 and MyD88-dependent signaling pathway. J. Immunol. *182*, 851–859.

472 Arnaud, M., Chastanet, A., and Débarbouillé, M. (2004). New vector for efficient allelic
473 replacement in naturally nontransformable, low-GC-content, gram-positive bacteria. Appl.
474 Environ. Microbiol. *70*, 6887–6891.

475 Barabas, O. (2004). Structural insights into the catalytic mechanism of phosphate ester
476 hydrolysis by dUTPase. J. Biol. Chem. *279*, 42907–42915.

477 Behrends, C., Sowa, M.E., Gygi, S.P., and Harper, J.W. (2010). Network organization of
478 the human autophagy system. Nature *466*, 68–76.

479 Blagoev, B., Kratchmarova, I., Ong, S.-E., Nielsen, M., Foster, L.J., and Mann, M. (2003).
480 A proteomics strategy to elucidate functional protein-protein interactions applied to EGF
481 signaling. Nat. Biotechnol. *21*, 315–318.

482 Chan, S., Segelke, B., Lekin, T., Krupka, H., Cho, U.S., Kim, M.-Y., So, M., Kim, C.-Y.,
483 Naranjo, C.M., and Rogers, Y.C. (2004). Crystal Structure of the *Mycobacterium*
484 *tuberculosis* dUTPase: Insights into the Catalytic Mechanism. J. Mol. Biol. *341*, 503–517.

485 Charpentier, E., Anton, A.I., Barry, P., Alfonso, B., Fang, Y., and Novick, R.P. (2004).
486 Novel cassette-based shuttle vector system for gram-positive bacteria. Appl. Environ.
487 Microbiol. *70*, 6076–6085.

488 Chen, J., and Novick, R.P. (2009). Phage-mediated intergeneric transfer of toxin genes.
489 Science *323*, 139–141.

490 Chu, R., Lin, Y., Rao, M.S., and Reddy, J.K. (1996). Cloning and identification of rat
491 deoxyuridine triphosphatase as an inhibitor of peroxisome proliferator-activated receptor
492 alpha. J. Biol. Chem. *271*, 27670–27676.

493 Dubrovay, Z. (2004). Multidimensional NMR identifies the conformational shift essential
494 for catalytic competence in the 60-kDa *Drosophila melanogaster* dUTPase trimer. J. Biol.
495 Chem. *279*, 17945–17950.

496 Etienne-Manneville, S., and Hall, A. (2002). Rho GTPases in cell biology. Nature *420*,
497 629–635.

498 Ewing, R.M., Chu, P., Elisma, F., Li, H., Taylor, P., Climie, S., McBroom-Cerajewski, L.,
499 Robinson, M.D., O'Connor, L., Li, M., et al. (2007). Large-scale mapping of human
500 protein-protein interactions by mass spectrometry. Mol. Syst. Biol. *3*, 89.

501 Freeman, L., Buisson, M., Tarbouriech, N., Van der Heyden, A., Labbe, P., and
502 Burmeister, W.P. (2009). The flexible motif V of Epstein-Barr virus deoxyuridine 5'-
503 triphosphate pyrophosphatase is essential for catalysis. J. Biol. Chem. *284*, 25280–25289.

504 Glaser, R., Litsky, M., Padgett, D., Baiocchi, R., Yang, E., Chen, M., Yeh, P.,
505 Greenchurch, K., Caligiuri, M., and Williams, M. (2006). EBV-encoded dUTPase induces
506 immune dysregulation: Implications for the pathophysiology of EBV-associated disease.
507 Virology *346*, 205–218.

508 Ho, Y., Gruhler, A., Heilbut, A., Bader, G.D., Moore, L., Adams, S.-L., Millar, A., Taylor, P.,
509 Bennett, K., Boutilier, K., et al. (2002). Systematic identification of protein complexes in
510 *Saccharomyces cerevisiae* by mass spectrometry. Nature *415*, 180–183.

511 Ito, T., Chiba, T., Ozawa, R., Yoshida, M., Hattori, M., and Sakaki, Y. (2001). A
512 comprehensive two-hybrid analysis to explore the yeast protein interactome. Proc. Natl.

513 Acad. Sci. U.S.A. *98*, 4569–4574.

514 Kim, D.-M., Chung, K.-S., Choi, S.-J., Jung, Y.-J., Park, S.-K., Han, G.-H., Ha, J.-S., Song,
515 K.-B., Choi, N.-S., Kim, H.-M., et al. (2009). RhoB induces apoptosis via direct interaction
516 with TNFAIP1 in HeLa cells. Int. J. Cancer *125*, 2520–2527.

517 Koehler, S.E., and Ladner, R.D. (2004). Small interfering RNA-mediated suppression of
518 dUTPase sensitizes cancer cell lines to thymidylate synthase inhibition. Mol. Pharmacol.
519 *66*, 620–626.

520 Kouzminova, E.A., and Kuzminov, A. (2004). Chromosomal fragmentation in dUTPase-
521 deficient mutants of *Escherichia coli* and its recombinational repair. Mol. Microbiol. *51*,
522 1279–1295.

523 Leang, R.S., Wu, T.-T., Hwang, S., Liang, L.T., Tong, L., Truong, J.T., and Sun, R. (2011).
524 The anti-interferon activity of conserved viral dUTPase ORF54 is essential for an effective
525 MHV-68 infection. PLoS Pathog *7*, e1002292.

526 Madrid, A.S., and Ganem, D. (2012). Kaposi's sarcoma-associated Herpesvirus
527 ORF54/dUTPase downregulates a ligand for the NK activating receptor NKp44. J. Virol.
528 *86*, 8693–8704.

529 Maiques, E., Ubeda, C., Tormo, M.A., Ferrer, M.D., Lasa, I., Novick, R.P., and Penadés,
530 J.R. (2007). Role of staphylococcal phage and SaPI integrase in intra- and interspecies
531 SaPI transfer. J. Bacteriol. *189*, 5608–5616.

532 Maul, R.W., Saribasak, H., Martomo, S.A., McClure, R.L., Yang, W., Vaisman, A.,
533 Gramlich, H.S., Schatz, D.G., Woodgate, R., Wilson, D.M., et al. (2011). Uracil residues
534 dependent on the deaminase AID in immunoglobulin gene variable and switch regions.
535 Nature *12*, 70–76.

536 Muha, V., Horváth, A., Békési, A., Pukáncsik, M., Hodoscsek, B., Merényi, G., Róna, G.,
537 Batki, J., Kiss, I., Jankovics, F., Vilmos, P., Erdélyi, M., and Vértessy, B.G. (2012). Uracil-
538 containing DNA in *Drosophila*: stability, stage-specific accumulation, and developmental
539 involvement. PLos Genet. 8(6):e1002738.

540 Novick, R.P., Christie, G.E., and Penadés, J.R. (2010). The phage-related chromosomal
541 islands of Gram-positive bacteria. Nat. Rev. Microbiol. *8*, 541–551.

542 Petersen-Mahrt, S.K., Harris, R.S., and Neuberger, M.S. (2002). AID mutates *E. coli*
543 suggesting a DNA deamination mechanism for antibody diversification. Nature *418*, 99–
544 103.

545 Pécsi, I., Hirmondo, R., Brown, A.C., Lopata, A., Parish, T., Vertessy, B.G., and Tóth, J.
546 (2012). The dUTPase enzyme is essential in *Mycobacterium smegmatis.* PLoS One 7(5):
547 e37461.

548 Pécsi, I., Szabó, J.E., Adams, S.D., Simon, I., Sellers, J.R., Vértessy, B.G., and Tóth, J.
549 (2011). Nucleotide pyrophosphatase employs a P-loop-like motif to enhance catalytic
550 power and NDP/NTP discrimination. Proc. Natl. Acad. Sci. U.S.A. *108*, 14437–14442.

551 Tchigvintsev, A., Singer, A.U., Flick, R., Petit, P., Brown, G., Evdokimova, E., Savchenko,
552 A., and Yakunin, A.F. (2011). Structure and activity of the *Saccharomyces cerevisiae*
553 dUTP pyrophosphatase DUT1, an essential housekeeping enzyme. Biochem. J. *437*,
554 243–253.

555 Tormo-Más, M.Á., Mir, I., Shrestha, A., Tallent, S.M., Campoy, S., Lasa, Í., Barbé, J.,
556 Novick, R.P., Christie, G.E., and Penadés, J.R. (2010). Moonlighting bacteriophage
557 proteins derepress staphylococcal pathogenicity islands. Nature *465*, 779–782.

558 Úbeda, C., Barry, P., Penadés, J.R., and Novick, R.P. (2007). A pathogenicity island
559 replicon in *Staphylococcus aureus* replicates as an unstable plasmid. Proc. Natl. Acad.
560 Sci. U.S.A. *104*, 14182–14188.

561 Úbeda, C., Maiques, E., Barry, P., Matthews, A., Tormo, M.Á., Lasa, Í., Novick, R.P., and
562 Penadés, J.R. (2008). SaPI mutations affecting replication and transfer and enabling
563 autonomous replication in the absence of helper phage. Mol. Microbiol. *67*, 493–503.

564 Varga, B., Barabás, O., Kovári, J., Tóth, J., Hunyadi-Gulyás, É., Klement, É.,
565 Medzihradszky, K.F., Tölgyesi, F., Fidy, J., and Vértessy, B.G. (2007). Active site closure
566 facilitates juxtaposition of reactant atoms for initiation of catalysis by human dUTPase.
567 FEBS Lett. *581*, 4783–4788.

568 Vertessy, B.G. (1997). Flexible glycine rich motif of Escherichia coli deoxyuridine
569 triphosphate nucleotidohydrolase is important for functional but not for structural integrity
570 of the enzyme. Proteins *28*, 568–579.

571 Vertessy, B.G., Larsson, G., Persson, T., Bergman, A.C., Persson, R., and Nyman, P.O.
572 (1998). The complete triphosphate moiety of non-hydrolyzable substrate analogues is
573 required for a conformational shift of the flexible C-terminus in *E. coli* dUTP
574 pyrophosphatase. FEBS Lett. *421*, 83–88.

575 Vetter, I.R., and Wittinghofer, A. (2001). The guanine nucleotide-binding switch in three
576 dimensions. Science *294*, 1299–1304.

577 Vértessy, B.G., and Tóth, J. (2009). Keeping uracil out of DNA: physiological role,
578 structure and catalytic mechanism of dUTPases. Acc. Chem. Res. *42*, 97–106.

579 Whittingham, J.L., Leal, I., Nguyen, C., Kasinathan, G., Bell, E., Jones, A.F., Berry, C.,
580 Benito, A., Turkenburg, J.P., Dodson, E.J., et al. (2005). dUTPase as a platform for
581 antimalarial drug design: structural basis for the selectivity of a class of nucleoside
582 inhibitors. Structure *13*, 329–338.

583 Williams, D., Norman, G., Khoury, C., Metcalfe, N., Briard, J., Laporte, A., Sheibani, S.,
584 Portt, L., Mandato, C.A., and Greenwood, M.T. (2011). Evidence for a second messenger
585 function of dUTP during Bax mediated apoptosis of yeast and mammalian cells. Biochem.
586 Biophys. Acta *1813*, 315–321.

587 Yan, N., O'Day, E., Wheeler, L.A., Engelman, A., and Lieberman, J. (2011). HIV DNA is
588 heavily uracilated, which protects it from autointegration. Proc. Natl. Acad. Sci. U.S.A.
589 *108*, 9244–9249.

590 Yu, H., Braun, P., Yildirim, M.A., Lemmens, I., Venkatesan, K., Sahalie, J., Hirozane-
591 Kishikawa, T., Gebreab, F., Li, N., Simonis, N., et al. (2008). High-quality binary protein
592 interaction map of the yeast interactome network. Science *322*, 104–110.

593 **FIGURE LEGENDS**

594 **Figure 1. Induction of SaPIbov1 by different phage-encoded Dut proteins**

595 SaPIbov1 excision and replication after induction with $CdCl_2$ of cloned *dut* alleles (wt and
596 D81A) from phage ϕ11, ϕ71 and 80α. A non-lysogenic *S. aureus* strain carrying SaPIbov1
597 was complemented with pCN51 derivative plasmids expressing 3xFLAG-tagged Dut
598 proteins under inducing conditions from the cadmium dependent P*cad* promoter. One ml
599 of each culture (OD_{540}=0.3) was collected 2 h after treatment with $CdCl_2$ (ranging from
600 0.05 to 2 μM) and used to prepare standard minilysates, which were resolved on a 0.7%
601 agarose gel, Southern blotted and probed for SaPIbov1 DNA. The upper band is "bulk"
602 DNA, including chromosomal, phage and replicating SaPI. CCC indicates covalently
603 closed circular SaPIbov1 DNA. The lower panel is a western blot probed with antibody to
604 the FLAG tag carried by the Dut proteins. +: wt protein; -: D81A mutant.

605 **Figure 2. Effects of phage 80α Dut mutations on SaPI replication and transfer**

606 (A) SaPIbov1 excision and replication after induction of cloned *dut* alleles from phage
607 80α. A non-lysogenic derivative of strain RN4220 carrying SaPIbov1 was complemented
608 with pCN51 derivative plasmids expressing different 3xFLAG-tagged Dut proteins. One ml
609 of each culture (OD_{540}=0.3) was collected 2 h after treatment with 2 μM $CdCl_2$ and used to
610 prepare standard minilysates, which were resolved on a 0.7% agarose gel, Southern
611 blotted and probed for SaPIbov1 DNA. The upper band is "bulk" DNA, including
612 chromosomal, phage and replicating SaPI; covalently closed circular (CCC) molecules
613 indicate replicating SaPIbov1 DNA. In these experiments, as no helper phage was
614 present, the excised SaPI DNA appears as CCC molecules rather than the linear
615 monomers that are seen following helper phage-mediated induction and packaging. The
616 lower panel is a western blot probed with antibody to the FLAG tag carried by the Dut
617 proteins.

618 (B) Southern blot after induction of 80α mutant lysates. Samples were isolated for 60 min
619 after induction with mitomycin C of the different lysogenic strains carrying SaPIbov1
620 *tst*::*tet*M. The samples were separated on agarose and blotted with a SaPIbov1-specific
621 probe. The upper band is "bulk" DNA. The intermediate band is SaPI linear monomers

622 released from phage heads and the lower band corresponds to the CCC SaPI form. As
623 previously indicated, the lower panel is a western blot probed with antibody to the FLAG
624 tag carried by the phage-encoded Dut proteins.

625 (C) The figure shows the number of transductans (log_{10}) per ml of induced culture, using
626 RN4220 as recipient strain. The means of results from three independent experiments are
627 presented. The frequency observed in the D81A, D81N, Y84I and ∆motif V mutants is
628 typical of transfer by generalized transduction, and is not SaPI-specific.

629 **Figure 3**. **Structures of wild-type Dut80α in apo and dUMpNpp bound conformations**

630 (A) Overview of a dUMpNpp bound Dut80α protomer isolated form the trimeric complex.
631 The protein is organized around a distorted β-barrel core from which the motifs V and VI
632 (labelled) are projected. Bound nucleotide is shown as stick with atomic colouring (carbon,
633 nitrogen, oxygen and phosphorus in green, blue, red and orange, respectively).

634 (B) Top view of the protomer, rotated by 90º around the horizontal axis relative to the view
635 in (A).

636 (C) Trimeric (monomers in blue, yellow and pink) apo and dUMpNpp-bound forms of wild-
637 type Dut80α orientated as the monomer in (A). Both structures are virtually identical to
638 each other (r.m.s.d. of 0.58 Å, Table S3) as well as with other trimeric dUTPases (see
639 Figure S4) with the exception of a characteristic insertion (motif VI) in the top of the trimer,
640 highlighted with darker shade and indicated by a black star in the dUMpNpp trimer, that
641 generates a flat surface. In the nucleotide-bound form, each independent active site
642 contains a molecule of dUMpNpp represented and coloured as in (A). The active centre is
643 closed by the P-loop-like C-terminal motif V, highlighted in a darker shade and indicated
644 by a black arrow, which is only ordered when the nucleotide is bound in a catalytic
645 competent conformation (dUMpNpp form).

646 (D) Close view of the dUMpNpp bound active site. The five conserved motives in the
647 dUTPases and the additional insertional motif VI in phage dUTPases are coloured in

darker hues, and the dUTP interacting residues are shown as sticks with carbon atoms in the colour of the corresponding motif. Motif V covering the active centre is only visible when the catalytic water (cyan sphere) is coordinated by D81 in a catalytic competent conformation. The Mg ion chelated by the nucleotide is shown as a grey sphere.

(E) Close-up view of co-ordination of catalytic machinary in the active site of Dut80α. The nucleophilic water (cyan sphere) is placed to atack dUTP (sticks with green carbons) α-phosphate by a network of direct and indirect contacts. Dashed lines indicate the contacts and are colored as follow; direct nucleophilic water contacts (Black), D81 contacts (green) and contacts of other conserved residues (dark-red). Residues are shown in stick, colored according to its monomer and labelled. Mg is represented as a dark-green sphere.

Figure 4. Motifs V and VI in wild-type Dut80α and mutant forms

The structures of the wild-type and mutant forms of Dut80α are shown, from a top view, in cartoon form coloured by subunits. The conformation of the insertional motif VI, highlighted by a darker shade and indicated by a black star in the WT structure, is conserved in all the protein forms independently of mutations or the presence of nucleotides. In those structures, the ordered P-loop motif V is highlighted in a darker shade and indicated by black arrows. The partial ordered P-loop motif V of Y84A mutant is indicated by green arrows.

Figure 5. Global architecture and active centre of Dut80α mutants

(A) Cartoon representation of the trimeric Dut80α^{D81N}, Dut80α^{Y84F} and Dut80α$^{D81A\text{-}CC}$ mutant proteins (same view that Figure 3C) in complex with dUMpNpp, except for the Dut80α$^{D81A\text{-}CC}$ mutant, which showed a dUMP molecule in its active center. In those structures that the P-loop motif V was ordered is highlighted in a darker shade and indicated by black arrows. The disulphide bound in the Dut80α$^{D81A\text{-}CC}$ mutant is indicated by a cyan arrow.

(B) Closed-view of the active centres. The nucleotide and the interacting residues are

shown in stick with atomic colouring (carbons in green for the nucleotide and in the colour of the corresponding protomer for the residues). The Cys residues (C110-C168) forming the disulphide bound in Dut80α$^{D81A-CC}$ are shown in stick with the sulphur atoms in cyan.

Figure 6. Derepression of *str* transcription by *dut* expression

(A) Schematic representation of the *bla*Z transcriptional fusion generated in plasmid pJP674. Strains containing pJP674- and pCN51-derivative plasmids expressing the different 80α *dut* alleles were assayed for β-lactamase activity after induction with 2 μM $CdCl_2$. Samples were normalized for total cell mass. Values presented are the averages (±SD) of three independent assays.

(B) Growth phase analysis of *S. aureus* strains after induction of cloned *dut* alleles from phage 80α. A non-lysogenic derivative of strain RN4220 carrying SaPIbov1 was complemented with pCN51 derivative plasmids expressing different Dut80α proteins (wt, D81A or D81A D110C-S168C). The bacteria were cultured in LB (with 0.1 μM $CdCl_2$) on a rotary shaker at 37°C. At the time indicated, the optical density of the culture was determined at 540 nm. Values presented are the averages (±SD) of three independent assays.

Figure 7. Schematic diagram of dUTPase activities

Top, dUTP is degraded to dUMP and pyrophosphate by the canonical activity of dUTPases (a). The binding of the dUTP in a catalytic competent conformation implicated the P-loop motif V in stabilisation, allowing the in-line attack of the α phosphate by the catalytic water (cyan) that is placed and activated by a conserved aspartic residue (D). The hydrolysis of α-β bound phosphate induces a conformational change of the nucleotide that destabilizes the P-loop motif V and allows the release of products (dUMP and PPi). Bottom, dUTPases present a G-like signalling activity. The dUTP-bound form is recognized by the target protein using the extra domain VI and the P-loop motif V as a switch (b). The release of the nucleotide and pyrophosphate after dUTP hydrolysis (c)

allows the P-loop switch region to relax into a disordered conformation that induces the target liberation.

Tables

Table 1. Crystallographic statistics for WT and mutant Dut80α proteins.

	Dut80wt dUMpNpp	**Dut80wt Apo**	**Dut80^{D81A} dUMpNpp**	**Dut80^{D81N} dUMpNpp**	**Dut80^{Y84I}**	**Dut80^{Y84A} dUMpNpp**	**Dut80^{Y84F} dUMpNpp**	**Dut80$^{D81A\text{-}CC}$ dUMP**
Data Collection								
Beamline	ESRF-ID23.1	DLS-I04-1	DLS-I04-1	DLS-I04-1	DLS-I04-1	DLS-I04-1	In home	ESRF-ID23.2
Wavelength (Å)	0.9334	0.9173	0.9334	0.9334	0.9795	0.9795	1.54	0.8726
Space group	$P2_13$	$P2_13$	$P2_13$	$P2_13$	$P2_13$	$P2_13$	$P2_13$	$P2_13$
Cell dimensions (Å)	a = 88.66	a = 87.37	a = 87.12	a = 87.21	a = 87.18	a = 87.47	a = 88.24	a = 87.46
Resolution (Å)[a]	44.3 – 2.8 (2.95 - 2.8)	50.4 – 2.9 (3.06 - 2.9)	50.3 – 2.9 (3.06 – 2.9)	50.4 – 3.0 (3.16 – 3.0)	61.7 – 3.1 (3.27 – 3.1)	61.9 – 3.1 (3.27 – 3.1)	14.9 – 3.0 (3.16 – 3.0)	39.11 – 2.60 (2.74 – 2.60)
Unique reflections	5949 (849)	5142 (744)	5103 (722)	4611 (666)	4199 (601)	4224 (600)	4719 (682)	7102 (1028)
Completeness (%)	99.9 (100)	100 (100)	99.9 (100)	99.7 (100)	99.9 (100)	99.7 (100)	98.5 (100)	99.9 (100)
Multiplicity	6.1	9.2	8.1	7.4	5.2	5.3	4.4	5.7
I/σ(I)	11.2 (2.1)	8.7 (1.9)	6.8 (2.1)	7.6 (2.2)	6.8 (2.6)	8.2 (2.4)	7.5 (2.3)	23.2 (3.9)
Rmerge	0.067 (0.375)	0.080 (0.402)	0.068 (0.352)	0.083 (0.333)	0.084 (0.295)	0.062 (0.326)	0.166 (0.348)	0.047 (0.403)
Refinement								
R_{work}	0.217	0.212	0.242	0.230	0.232	0.240	0.222	0.224
R_{free}	0.264	0.252	0.275	0.285	0.278	0.291	0.277	0.273
Number of atoms								
Protein	1317	1238	1177	1244	1234	1279	1316	1329
Ligand	28	-	28	28	-	28	28	20
Water	67	41	31	39	27	12	34	51
Others	8	18	2	2	2	3	3	2
RMSD, bonds (Å)	0.0039	0.0046	0.0057	0.0051	0.0041	0.0041	0.0039	0.0046
RMSD, angles (°)	1.021	0.8166	0.9960	0.9610	0.7825	0.9221	0.8581	0.8691
Ramachandran plot:								
Preferred (%)	100	97.39	97.24	95.39	96.73	93.67	96.41	93.59
Allowed (%)		2.61	2.76	3.95	3.27	5.06	3.59	4.49

[a]Numbers in parentheses indicate values for the highest resolution cell

Figure 1

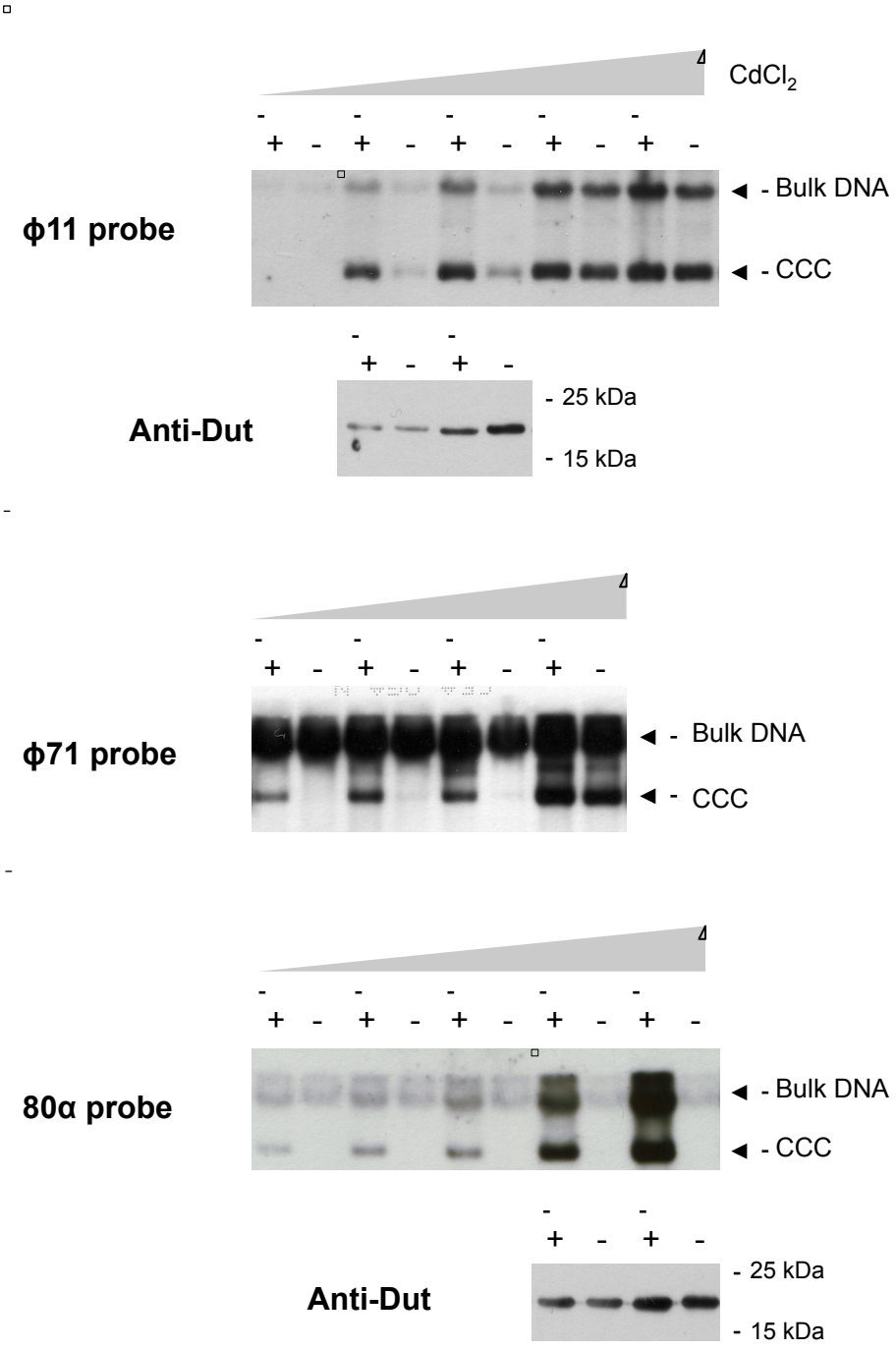
CdCl2
ϕ11 probe
- Bulk DNA
- CCC
Anti-Dut
- 25 kDa
- 15 kDa
ϕ71 probe
- Bulk DNA
- CCC
80α probe
- Bulk DNA
- CCC
Anti-Dut
- 25 kDa
- 15 kDa

Figure 2

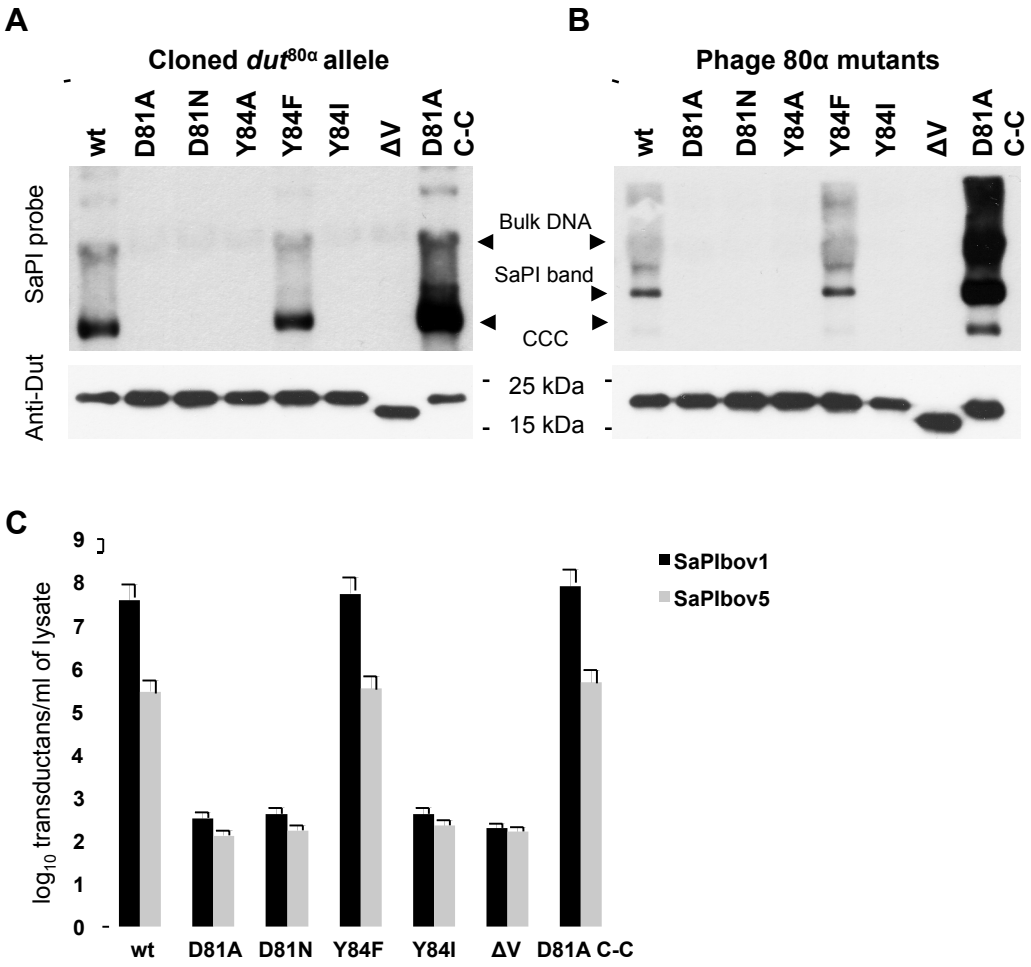
A
Cloned dut80α allele
wt
D81A
D81N
Y84A
Y84F
Y84I
ΔV
D81A C-C
SaPI probe
Anti-Dut
Bulk DNA
SaPI band
CCC
25 kDa
15 kDa
B
Phage 80α mutants
C
log10 transductans/ml of lysate
SaPIbov1
SaPIbov5

Figure 3

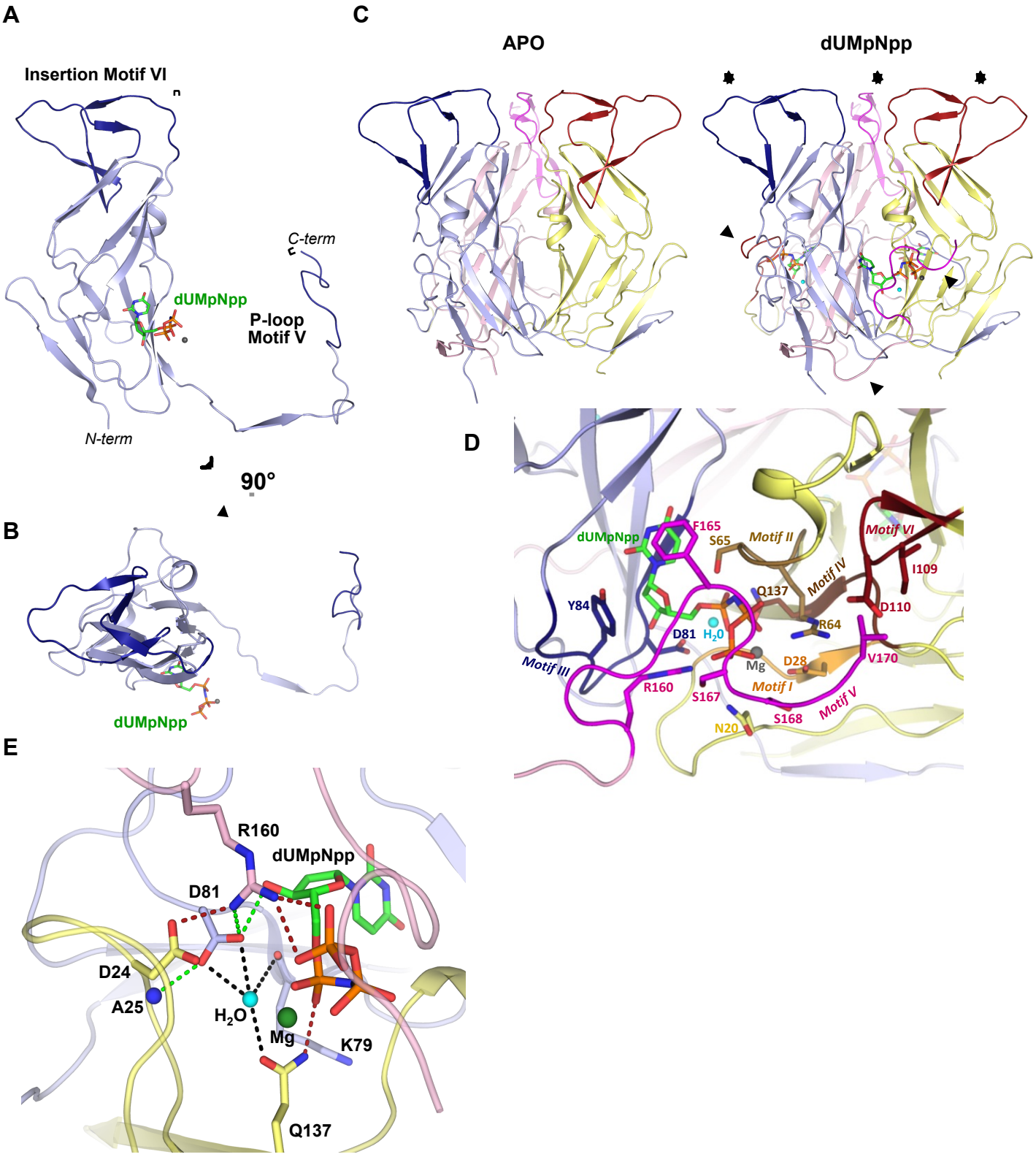
A
Insertion Motif VI
N
C-term
C
dUMpNpp
P-loop
Motif V
N-term
90°
B
dUMpNpp
C
APO
dUMpNpp
D
dUMpNpp
F165
S65
Motif II
Motif VI
I109
Y84
Q137
Motif IV
D110
D81
H2O
R64
Motif III
Mg
D28
V170
R160
S167
Motif I
Motif V
S168
N20
E
R160
dUMpNpp
D81
D24
A25
H2O
Mg
K79
Q137

Figure 4

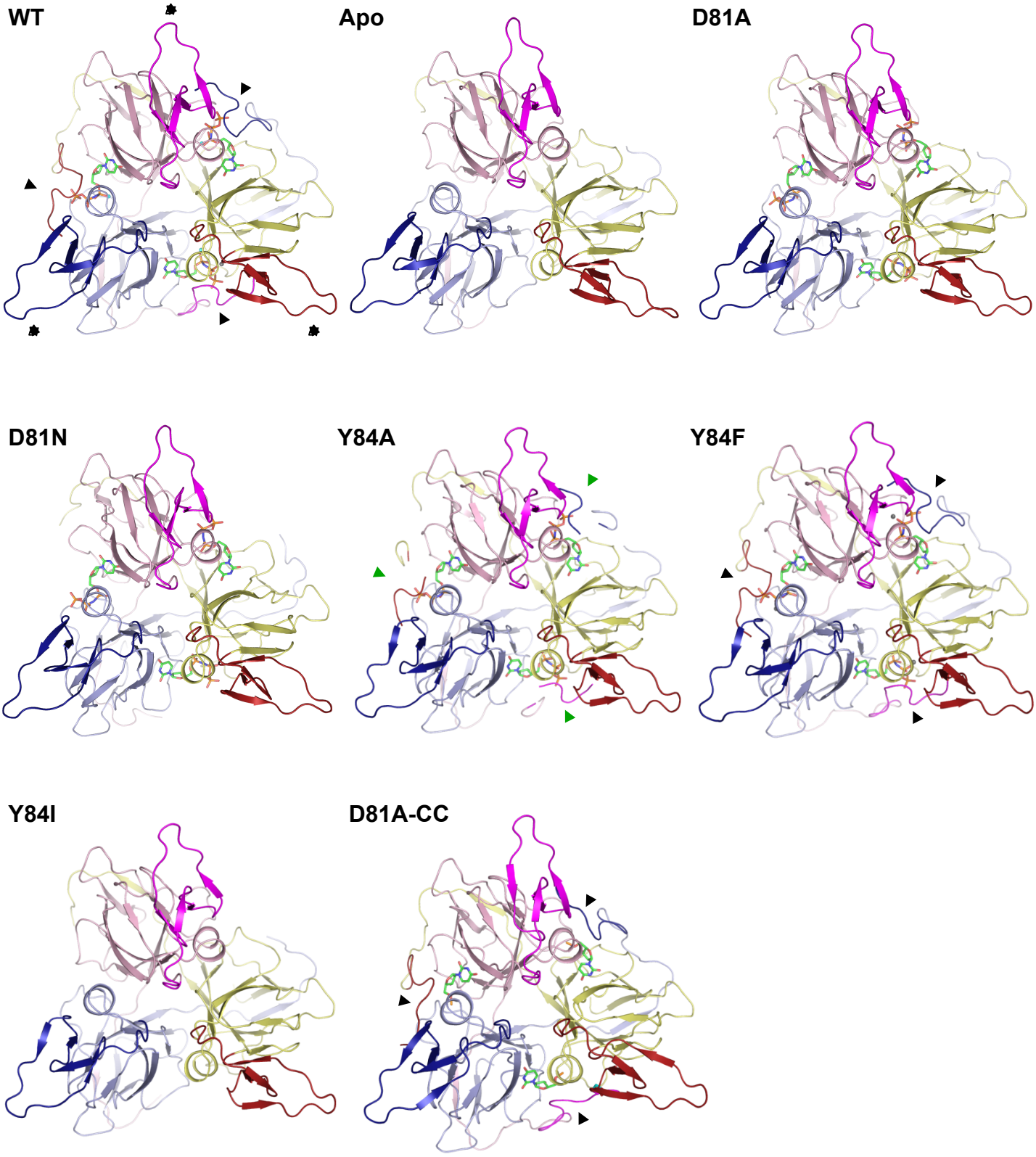

Figure 5

D81N

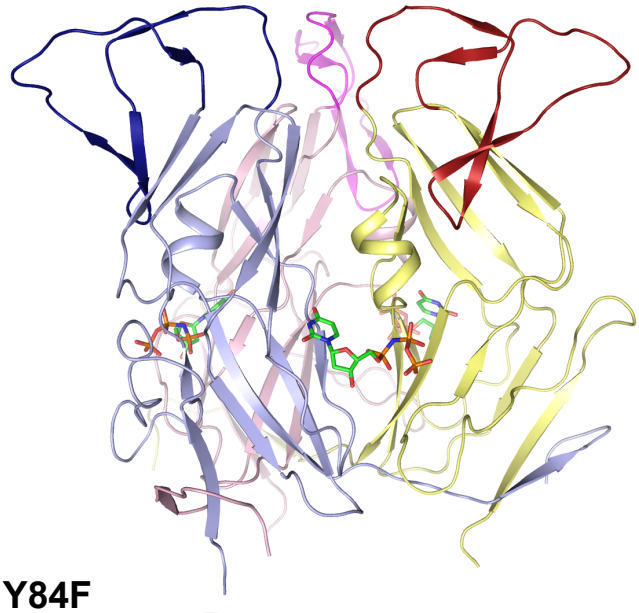

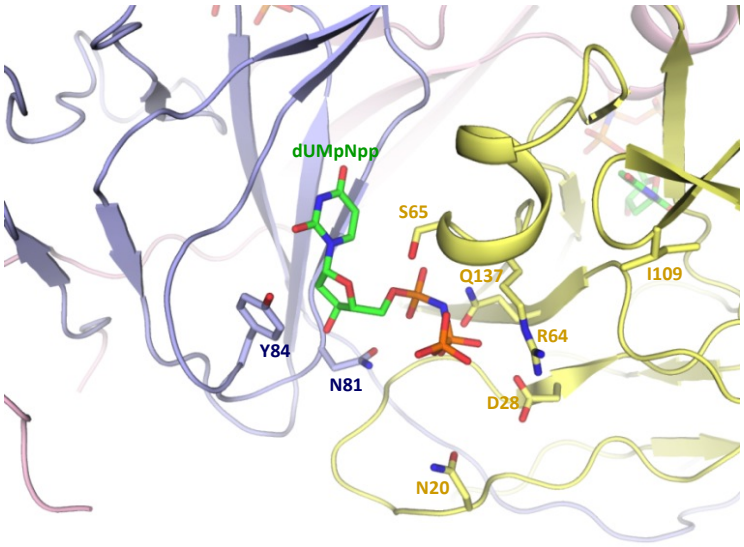

Y84F

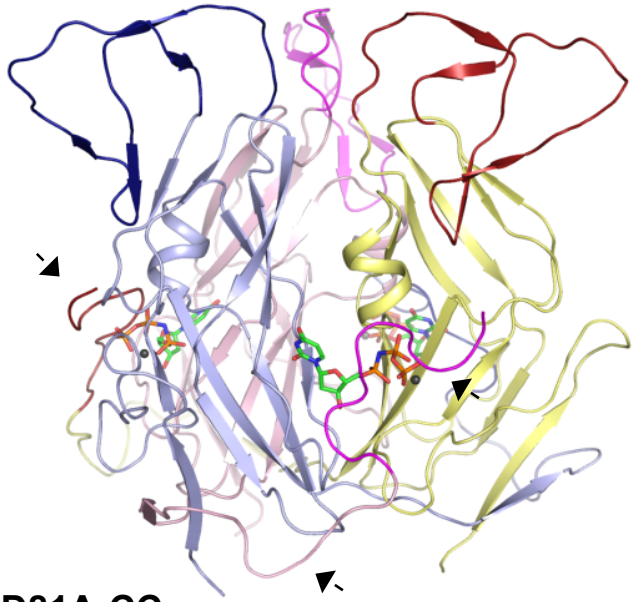

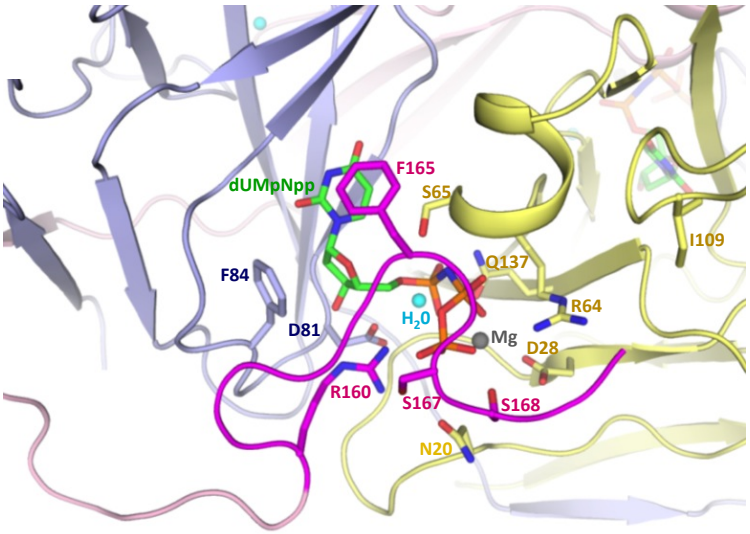

D81A-CC

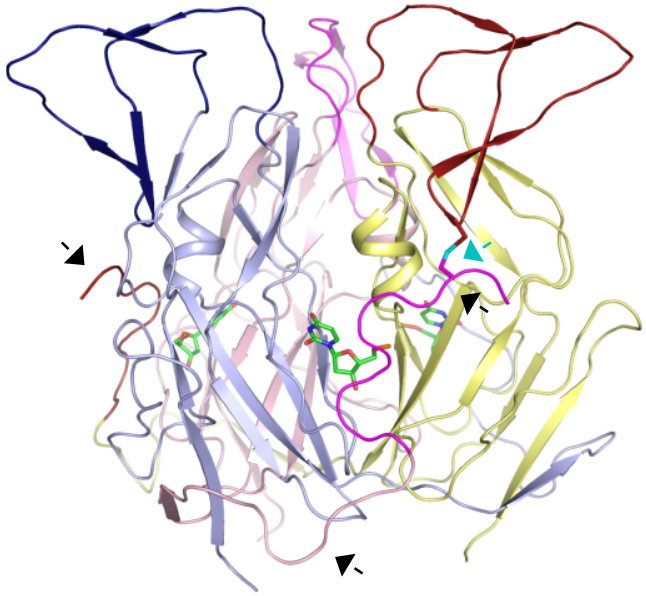

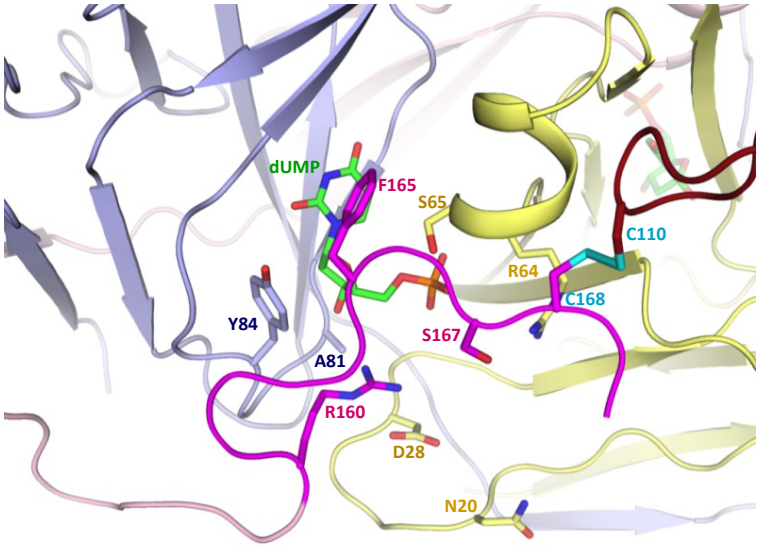

Figure 6

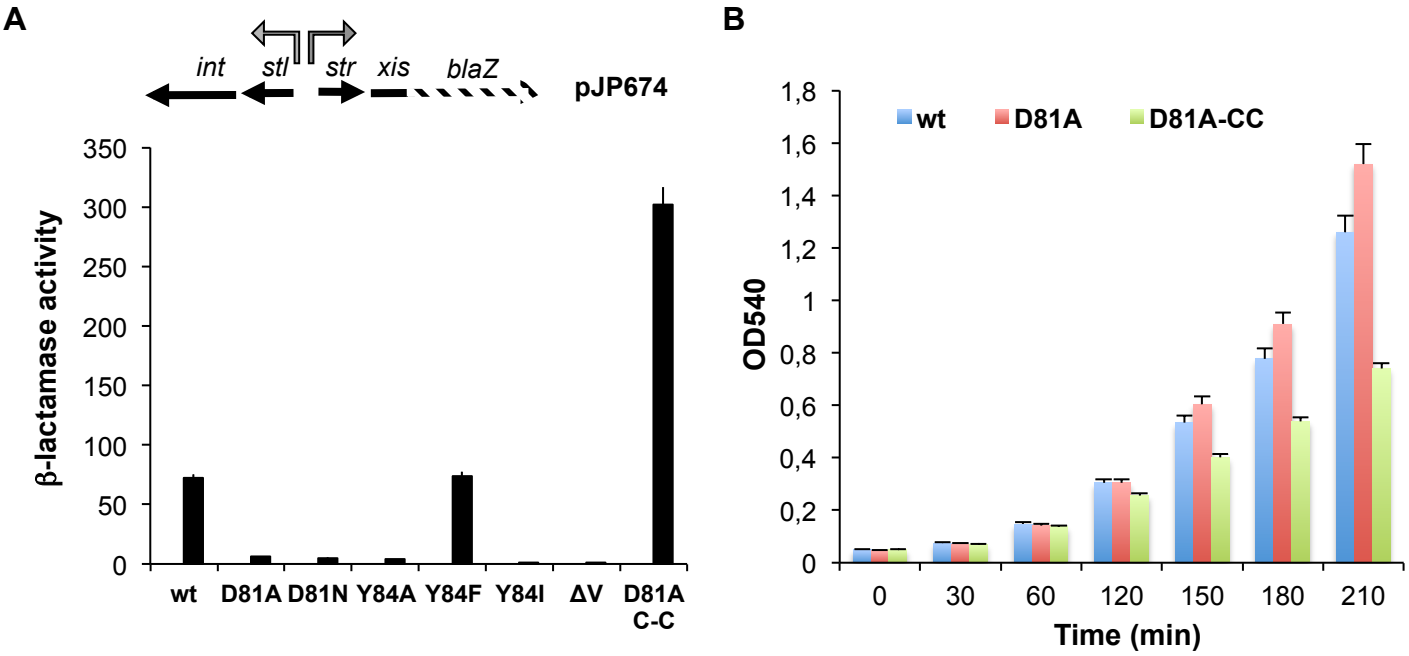
A
int
stI
str
xis
blaZ
pJP674
β-lactamase activity
350
300
250
200
150
100
50
0
wt
D81A
D81N
Y84A
Y84F
Y84I
ΔV
D81A C-C
B
wt
D81A
D81A-CC
OD540
1,8
1,6
1,4
1,2
1
0,8
0,6
0,4
0,2
0
0
30
60
120
150
180
210
Time (min)

Figure 7

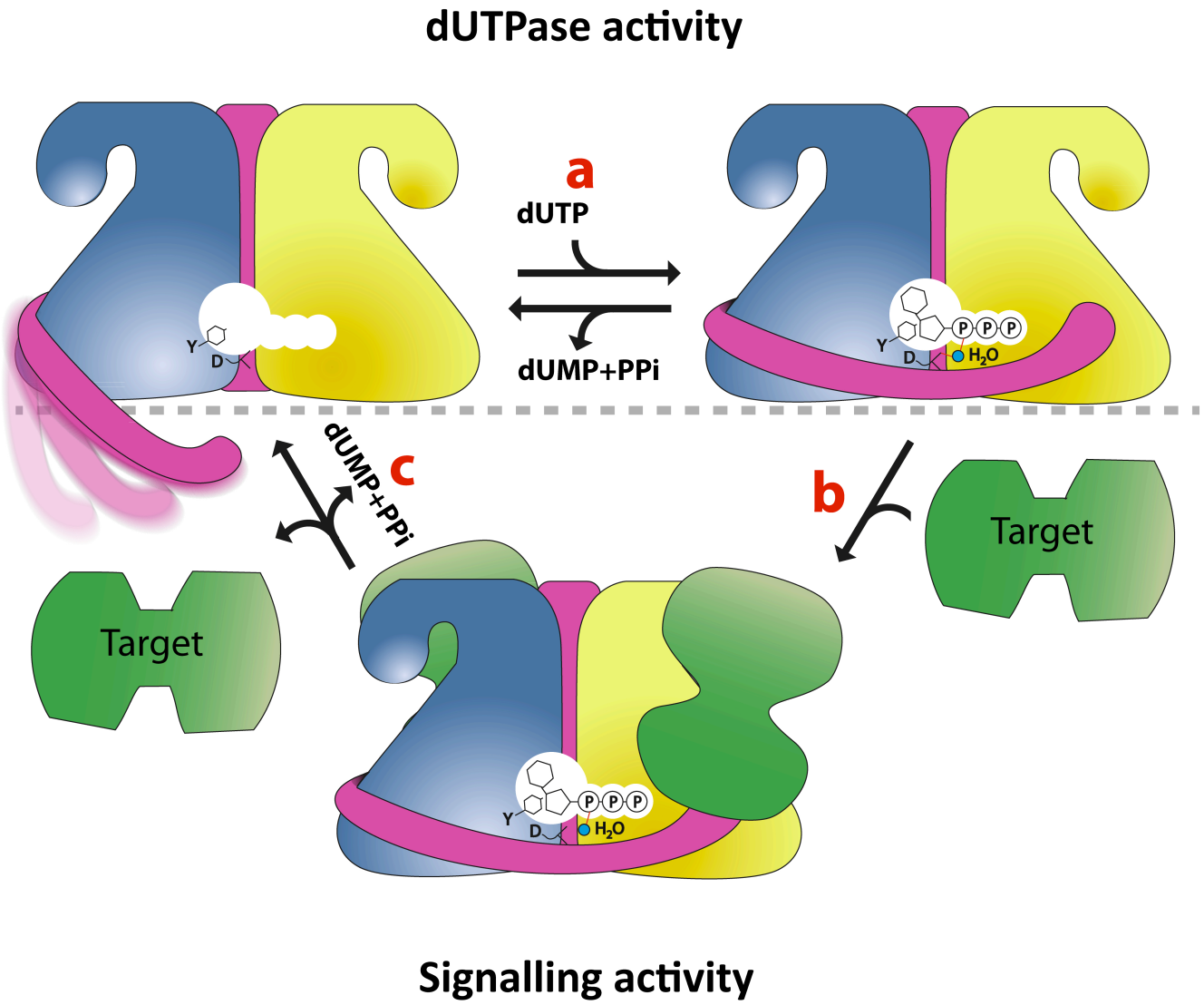
dUTPase activity
a
dUTP
dUMP+PPi
Y
D
P P P
H_2O
b
Target
c
dUMP+PPi
Target
Signalling activity

Molecular Cell

Supplemental Information

Phage dUTPases control transfer of virulence genes by a proto-oncogenic G protein-like mechanism

María Ángeles Tormo-Más, Jorge Donderis, María García-Caballer, Aaron Alt, Ignacio Mir-Sanchis, Alberto Marina, José R Penadés

Inventory of Supplemental Information

Figure S1, related to Figures 3-5.

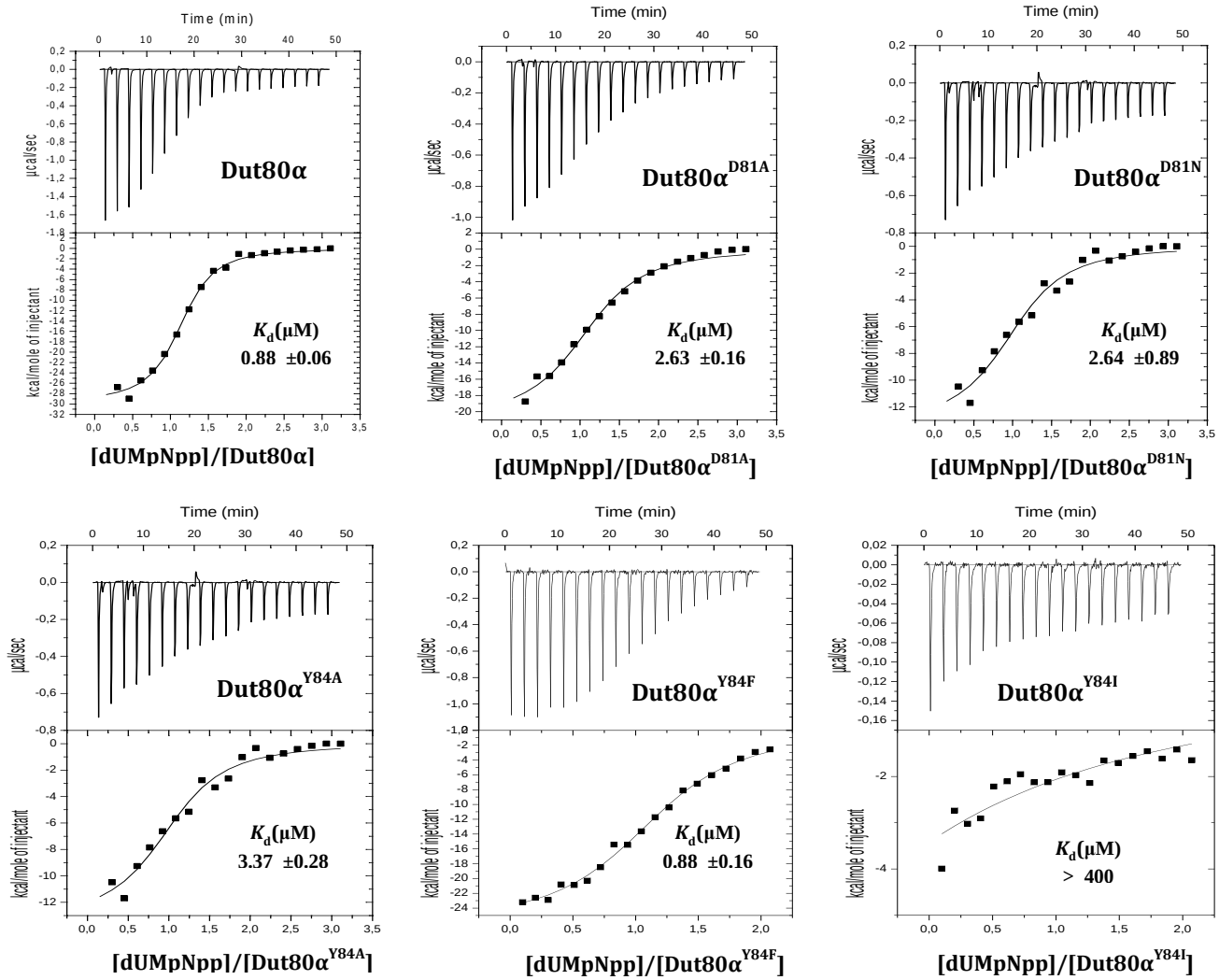

Figure S1. Effect of mutations on nucleotide binding.

ITC experiments on wild-type Dut80α and different D81 and Y84 mutants with dUMpNpp. The *K*d calculated from the ITC experiments is indicated.

Figure S2, related to Figures 3-5.

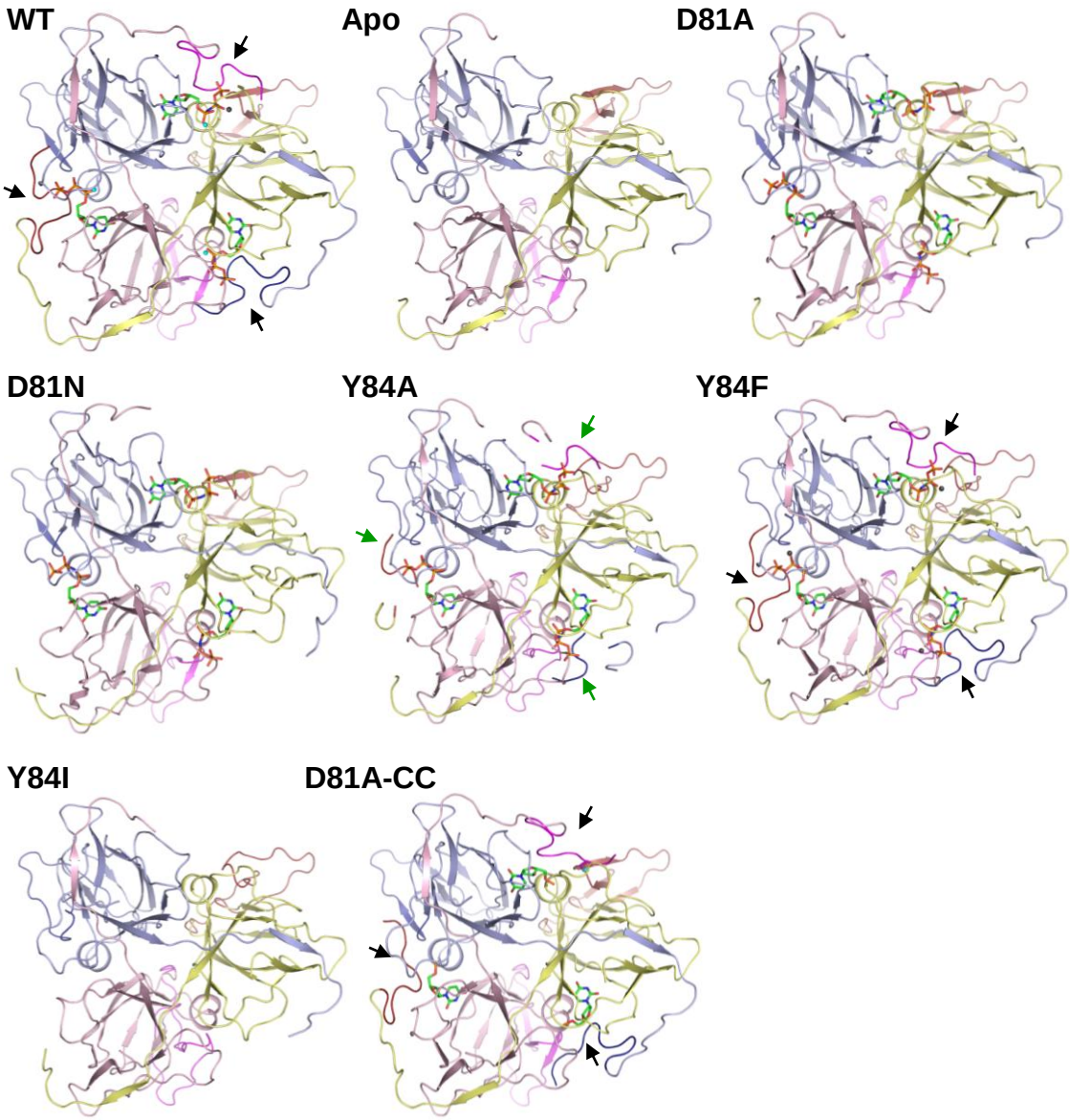

Figure S2. P-loop motif V in wild-type Dut80α and mutant forms.

The structures of the wild-type and mutant forms of Dut80α are shown, from a bottom view, in cartoon form coloured by subunits. When present, the nucleotide is shown in stick form with atomic colouring (carbons in green). In those structures, the ordered P-loop motif V is highlighted in a darker shade and indicated by black arrows. The partial ordered P-loop motif V of Y84A mutant is indicated by green arrows.

Figure S3, related to Figure 3.

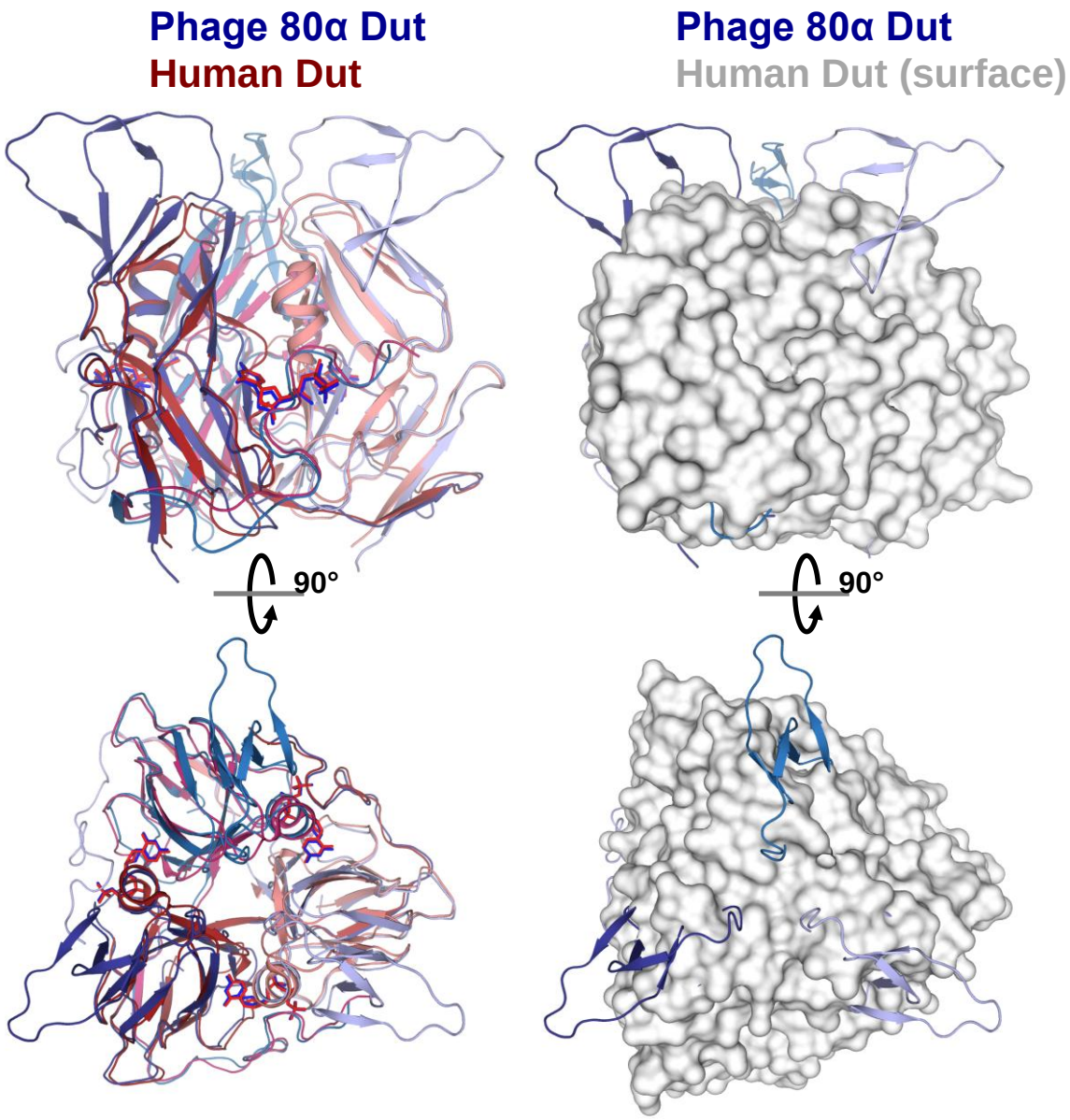

Figure S3. Structural comparison of Dut80α and human dUTPases.

The structure of Dut80α (blue) is virtually identical to that of human dUTPase (red, PDB 2HqU) (r.m.s.d. approximately 1 Å for the trimer), with quite similar disposition of their conserved motifs I-V (not shown), but presents a characteristic insertion (motif VI) in the top of the trimer, highlighted with a darker shade, that generates a flat surface. Two views (lateral and top) are shown: left, cartoon representation with the nucleotides in stick form; right, the human trimer is represented as a surface to highlight the Dut80α motif VI, displayed in cartoon form.

Figure S4, related to Figures 3-5.

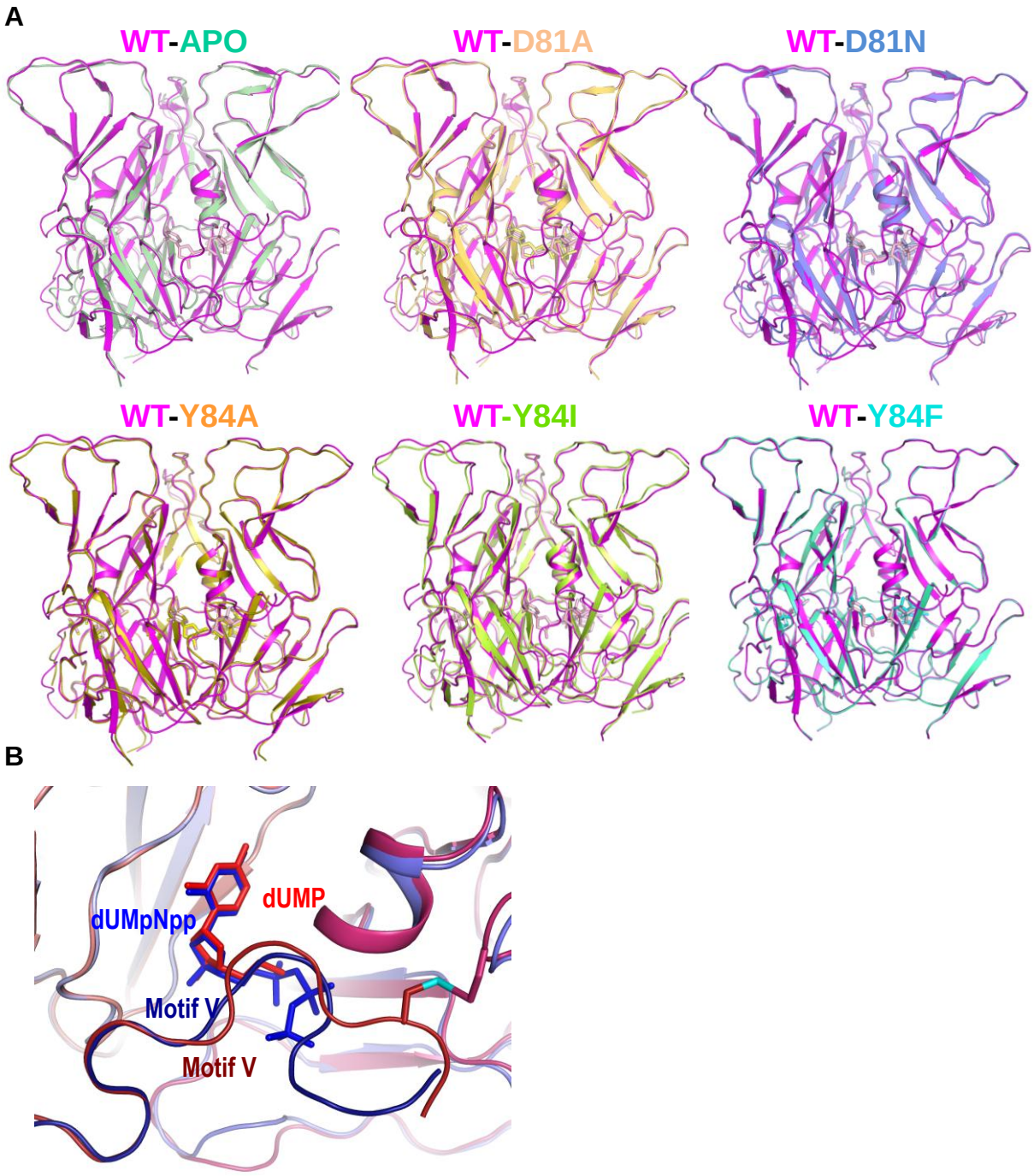

Figure S4.

(A) Superposition of nucleotide-bound wild-type Dut80α with mutant and apo forms.

The trimer forms were structural aligned onto dUMpNpp Dut80α (magenta). The nucleotides are shown as sticks and coloured according to the trimer.

(B) Nucleotide binding sites of wt Dut80α and Dut80α$^{D81A-CC}$ mutant.

Trimeric structures of wt Dut80α (hues of blue) and Dut80α$^{D81A-CC}$ (hues of red) were superimposed, and a close view of the one of the active center is shown. Despite D81 mutation in Dut80α$^{D81A-CC}$ and the presence of different nucleotides (dUMpNpp for wt Dut80α and dUMP for Dut80α$^{D81A-CC}$), motif V present a similar disposition in both structures except for the slight conformational differences in their last three residues. The nucleotides and the disulphide bond in Dut80α$^{D81A-CC}$ are represented in sticks.

Figure S5, related to Figures 4-5.

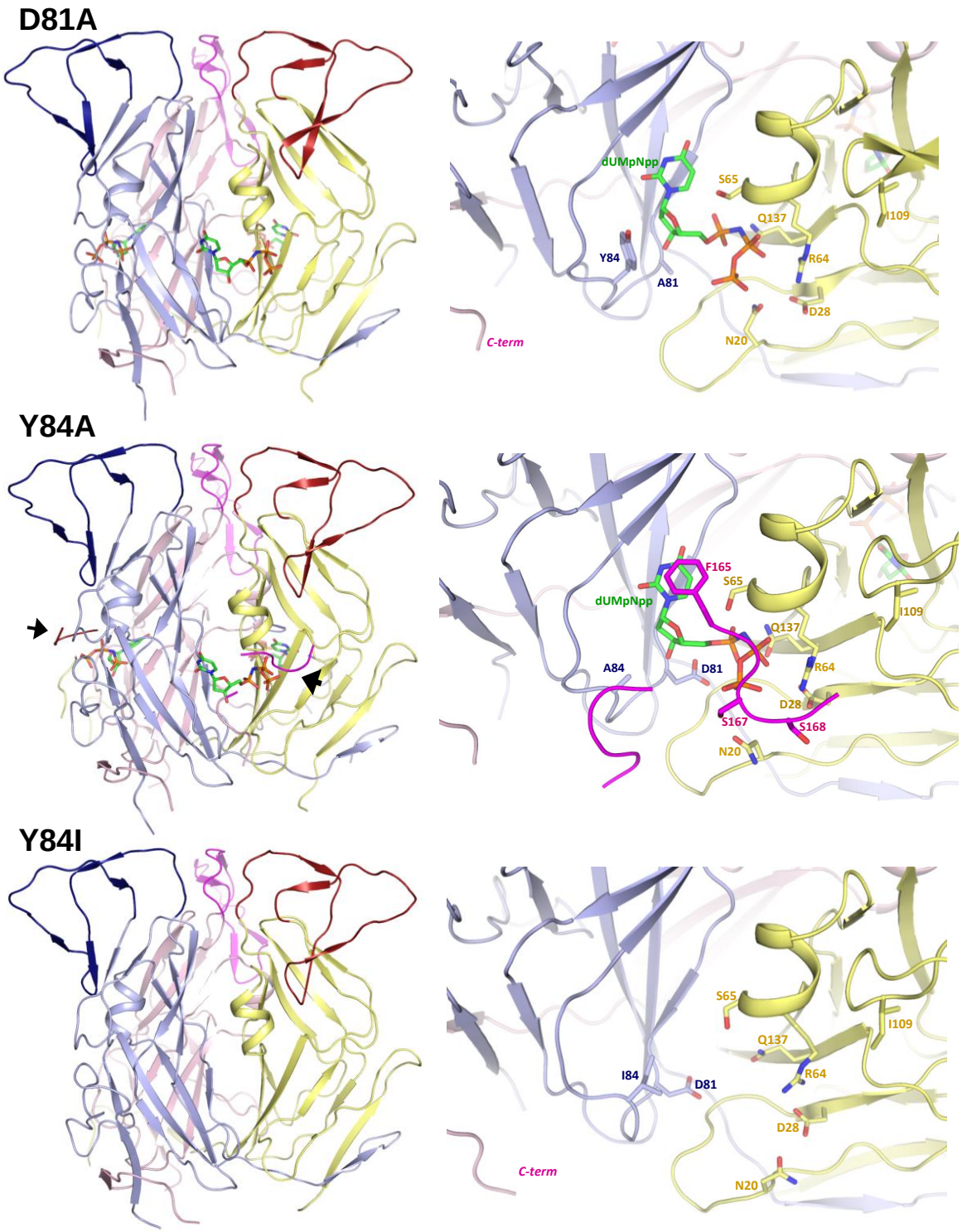

Figure S5. Global architecture and active centre of Dut80α mutants.

(A) Cartoon representation of the Dut80α^{D81A}, Dut80α^{Y84A} and Dut80α^{Y84I} mutant proteins in complex with dUMpNpp, except for the Dut80α^{Y84I} mutant, which does not bind the nucleotide analogue. The partial ordered P-loop motif V of Dut80α^{Y84A} mutant is indicated by black arrows.

(B) Closed-view of the active centres. The nucleotide and the interacting residues are shown in stick with atomic colouring (carbons in green for the nucleotide and in the colour of the corresponding protomer for the residues). In Dut80α^{Y84I} which active centre is empty, the conserved interacting residues are shown.

Figure S6, related to Figures 4-5.

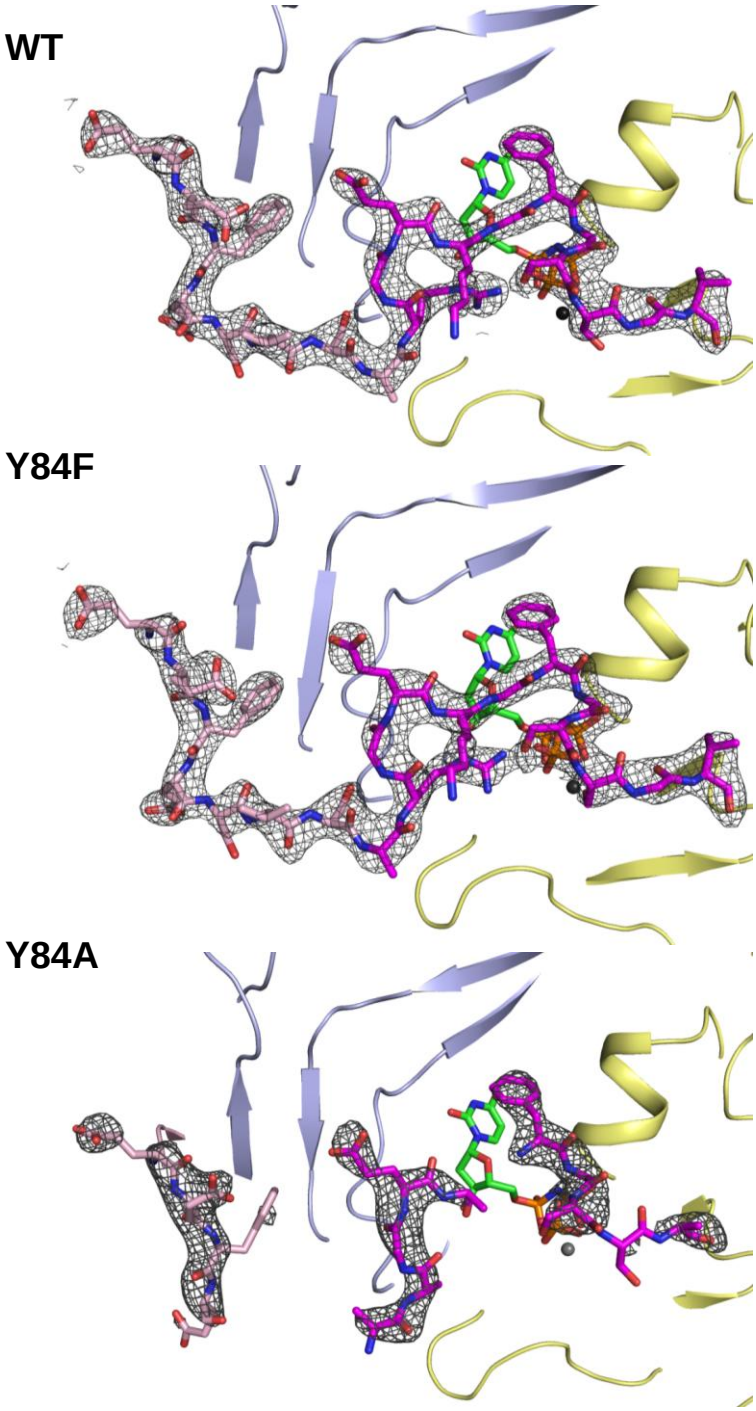

Figure S6. Motif V localization in wt Dut80α and Y84 mutants.

The modelled residues of the C-terminal end (152-170) are shown in stick model with atomic colouring and carbon atoms in different hues of pink. A dark shade is used for motif V (161-170) carbon atoms. The 2Fo–Fc maps used to model the structures are shown in grey and contoured at 1.5 σ level. The nucleotide is represented as sticks with atomic colouring (carbon, nitrogen, oxygen and phosphorus in green, blue, red and orange, respectively) and the rest of subunits are shown in ribbon representation (coloured blue and yellow).

Figure S7, related to points raised in the Discussion section.

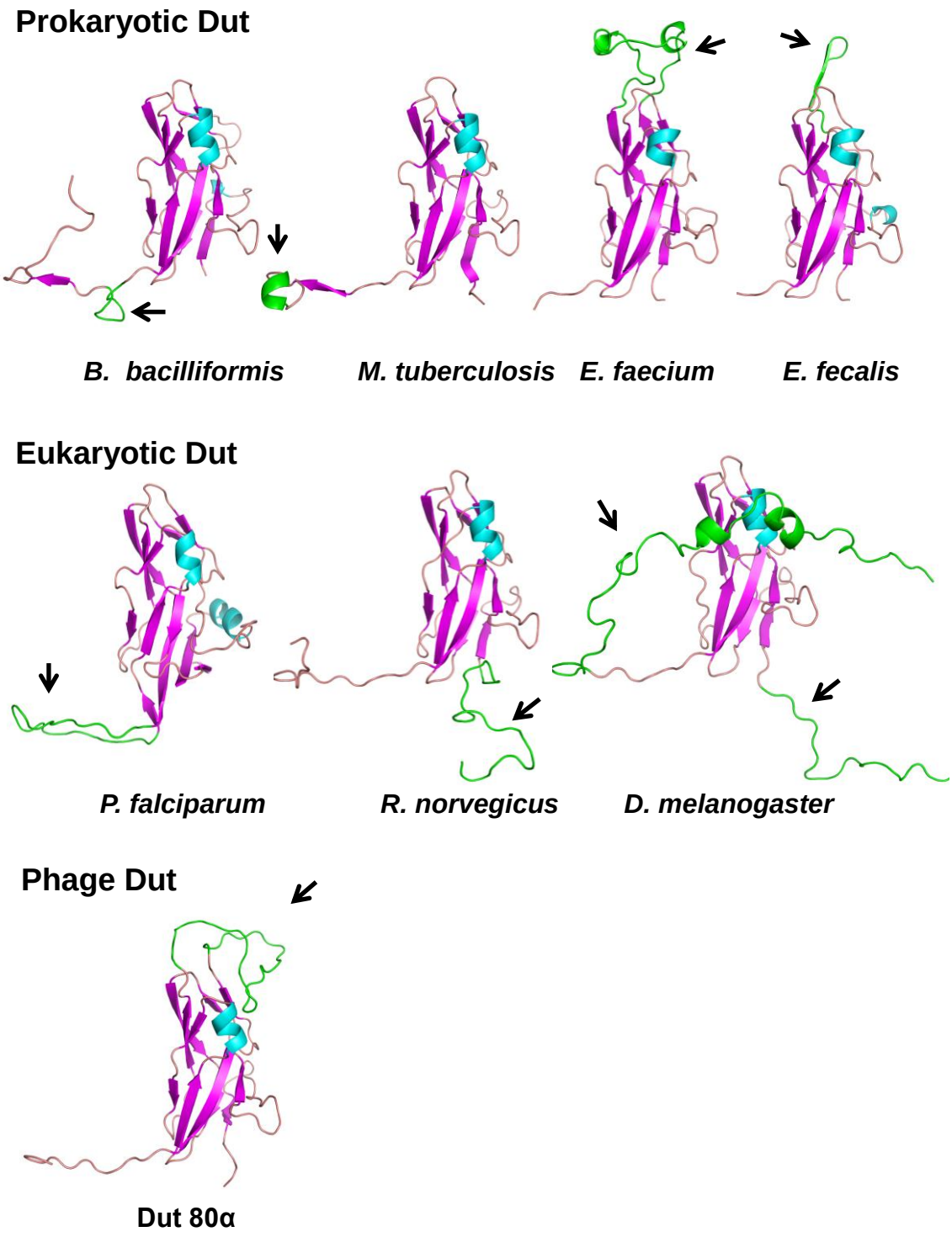

Figure S7. Monomeric structure of Dut proteins and localisation of the extra motif VI.

The structures of the *Mycobacterium tuberculosis*, *Plasmodium falciparum, Drosophila melanogaster* and staphylococcal 80α Dut proteins have been previously experimentally solved. *Bartonella bacilliformis* and enterococcal (*E. faecium* and *E. faecalis)* proteins were modelled against the *Brucella melitensis* and *Streptococcus mutants* Duts, respectively, using Swiss-Model server (http://swissmodel.expasy.org/workspace/). Rat Dut was modelled using SAM-T08 server (http://compbio.soe.ucsc.edu/SAM_T08/T08-query.html). The conformation of the insertional motif VI is highlighted in green and pointed out by black arrows. Note that the extra domains are located in the N-terminal region (*Rattus*, *Plasmodium* and *Drosophila*), C-terminal region (*Bartonella*, *Mycobacterium* and *Drosophila*) or in the middle (staphylococcal and enterococcal) of the Dut proteins. Although with a different localisation, the extra motif VI from the *Rattus* and the *Mycobacterium* Duts are also involved in signalling.

Table S1. dUTPase activity.

Phage	Protein[a]	Activity (nM/min)[b]	Kd (μM)
80α	wt	1.81	0.88
80α	D81A	0	2.63
80α	D81N	0	2.64
80α	Y84A	0.44	3.37
80α	Y84F	1.40	0.88
80α	Y84I	0	> 400
80α	ΔV	0	ND
80α	D81A C-C	0	ND

[a] $His_{(6)}$-Dut protein purified.
[b] Measured as production of PPi, using 0.1 μg of purified protein. Variation was within ±5% in all cases.
ND: Not determined.

Table S2. RMSD values in Å (*lower part*) from the superposition of the indicated number of Cα-atoms with residues matches in brackets (*upper part*).

	Dut80α WT **dUMpNpp**	**Dut80α** WT **Apo**	**Dut80α** D81A **dUMpNpp**	**Dut80α** D81N **dUMpNpp**	**Dut80α** Y84F **dUMpNpp**	**Dut80α** Y84A **dUMpNpp**	**Dut80α** Y84I	**Dut80α** D81A-CC **dUMP**
Dut80α^{WT} dUMpNpp		154 (2-155)	154 (2-155)	155 (2-156)	169 (2-170)	159 (2-156/160-163)	155 (2-156)	165 (2-166)
Dut80α WT Apo	0.58		143 (2-19/25-150)	153 (2-154)	154 (2-155)	154 (2-155)	154 (2-155)	155 (2-156)
Dut80α D81A dUMpNpp	0.43	0.57		149 (2-150)	142 (2-19/25-159)	147 (2-19/25-150)	149 (2-150)	149 (2-19/25-155)
Dut80α D81N dUMpNpp	0.50	0.46	0.38		155 (2-156)	154 (2-155)	155 (2-156)	155 (2-156)
Dut80α Y84F dUMpNpp	0.46	0.62	0.46	0.53		158 (2-155/160-163)	155 (2-156)	165 (2-166)
Dut80α Y84A dUMpNpp	0.44	0.63	0.41	0.49	0.46		155 (2-156)	154 (2-155)
Dut80α Y84I	0.62	0.48	0.56	0.56	0.65	0.62		155 (2-156)
Dut80α D81A-CC dUMP	0.60	0.53	0.43	0.41	0.63	0.57	0.49	

Table S3. Strains and plasmids used in this study.

Strains	Description	Reference
RN4220	Restriction-defective derivate of RN450	Laboratory strain
RN450	NCTC8325 cured of φ11, φ12 and φ13	Laboratory strain
BL21(DE3)	*E. coli* expression strain	Stratagene
RN10359	RN450 80α	(Úbeda et al., 2007)
JP3603	RN10359 SaPIbov1 *tst*::*tet*M	(Tormo-Más et al., 2010)
JP7084	RN10359 SaPIbov5 *tet*M	This work
JP6774	RN4220 Δ*spa* SaPIbov1 *tst*::*tet*M	(Tormo-Más et al., 2010)
JP9338	RN450 Δ*spa* SaPIbov1 *tst*::*tet*M	This work
JP8255	JP3603 3xflag-*dut* 80α	This work
JP8256	JP3603 3xflag-*dut* $_{D81A}$ 80α	This work
JP8258	JP3603 3xflag-*dut* $_{D81N}$ 80α	This work
JP8941	JP3603 3xflag-*dut* $_{Y84A}$ 80α	This work
JP8257	JP3603 3xflag-*dut* $_{Y84I}$ 80α	This work
JP8766	JP3603 3xflag-*dut* $_{Y84F}$ 80α	This work
JP9051	JP3603 3xflag-*dut* $_{\Delta V}$ 80α	This work
JP9340	JP3603 3xflag-*dut* $_{D81A, D110C, S168C}$ 80α	This work
JP9016	JP7084 *dut* $_{D81A}$ 80α	This work
JP9017	JP7084 *dut* $_{D81N}$ 80α	This work
JP9018	JP7084 *dut* $_{Y84A}$ 80α	This work
JP9020	JP7084 *dut* $_{Y84I}$ 80α	This work
JP9019	JP7084 *dut* $_{Y84F}$ 80α	This work
JP9021	JP7084 *dut* $_{\Delta V}$ 80α	This work
JP9341	JP7084 *dut* $_{D81A, D110C, S168C}$ 80α	This work
JP5359	BL21(DE3) pJP753	(Tormo-Más et al., 2010)
JP8474	BL21(DE3) pJP1132	This work
JP8475	BL21(DE3) pJP1133	This work
JP9348	BL21(DE3) pJP1143	This work
JP9349	BL21(DE3) pJP1144	This work
JP9350	BL21(DE3) pJP1145	This work
JP9351	BL21(DE3) pJP1146	This work
JP8434	BL21(DE3) pJP1147	This work
JP9026	JP6774 pJP821	(Tormo-Más et al., 2010)
JP9027	JP6774 pJP1157	This work
JP9028	JP6774 pJP1158	This work
JP9029	JP6774 pJP985	This work
JP9030	JP6774 pJP982	This work
JP9031	JP6774 pJP983	This work
JP9032	JP6774 pJP1159	This work
JP9343	JP6774 pJP1160	This work

Strains	Description	Reference
JP9344	JP9338 pJP821	This work
JP9345	JP9338 pJP1157	This work
JP9040	JP9338 pJP812	This work
JP9041	JP9388 pJP1161	This work
JP9346	JP9388 pJP1162	This work
JP9347	JP9388 pJP1163	This work
JP9033	pJP674 pJP821	This work
JP9034	pJP674 pJP1157	This work
JP9035	pJP674 pJP1158	This work
JP9036	pJP674 pJP985	This work
JP9037	pJP674 pJP982	This work
JP9038	pJP674 pJP983	This work
JP9039	pJP674 pJP1159	This work
JP9342	pJP674 pJP1160	This work

Plasmids	Description	Reference
pMAD	Vector for efficient allelic replacement	(Arnaud et al., 2004)
pCN51	Expresion vector	(Charpentier et al., 2004)
pET28a	Expresion vector	Novagen
pRN8298	Expresion vector	(Charpentier et al., 2004)
pJP1156	pMAD-*dut*$_{D81A}$ 80α	This work
pJP943	pMAD-*dut*$_{D81N}$ 80α	This work
pJP972	pMAD-*dut*$_{Y84A}$ 80α	This work
pJP973	pMAD-*dut*$_{Y84I}$ 80α	This work
pJP974	pMAD-*dut*$_{Y84F}$ 80α	This work
pJP1141	pMAD-*dut*$_{\Delta V}$ 80α	This work
pJP1136	pMAD-*dut*$_{D81A,\ D110C,\ S168C}$ 80α	This work
pJP980	pMAD-3xflag-*dut* 80α	This work
pJP753	pET28a-*dut* 80α	(Tormo-Más et al., 2010)
pJP1132	pET28a-*dut*$_{D81A}$ 80α	This work
pJP1133	pET28a-*dut*$_{D81N}$ 80α	This work
pJP1143	pET28a-*dut*$_{Y84A}$ 80α	This work
pJP1144	pET28a-*dut*$_{Y84F}$ 80α	This work
pJP1145	pET28a-*dut*$_{Y84I}$ 80α	This work
pJP1146	pET28a-*dut*$_{\Delta V}$ 80α	This work
pJP1147	pET28a-*dut*$_{D81A,\ D110C,\ S168C}$ 80α	This work
pJP821	pCN51-3xflag-*dut* 80α	(Tormo-Más et al., 2010)
pJP1157	pCN51-3xflag-*dut*$_{D81A}$ 80α	This work
pJP1158	pCN51- 3xflag-*dut*$_{D81N}$ 80α	This work
pJP985	pCN51- 3xflag-*dut*$_{Y84A}$ 80α	This work
pJP982	pCN51- 3xflag-*dut*$_{Y84F}$ 80α	This work
pJP983	pCN51- 3xflag-*dut*$_{Y84I}$ 80α	This work
pJP1159	pCN51- 3xflag-*dut*$_{\Delta V}$ 80α	This work
pJP1160	pCN51- 3xflag-*dut*$_{D81A,\ D110C,\ S168C}$ 80α	This work
pJP812	pCN51- 3xflag-*dut* ϕ11	This work
pJP1161	pCN51- 3xflag-*dut*$_{D81A}$ ϕ11	This work
pJP1162	pCN51- 3xflag-*dut* ϕ71	This work
pJP1163	pCN51- 3xflag-*dut*$_{D81A}$ ϕ71	This work
pJP674	pRN8298-clor-pInt-20-19-18*bla*Z	(Tormo-Más et al., 2010)

Table S4. Oligonucleotides used in this study.

Plasmids	Oligonucleotides	Sequence (5´-3´)
pJP1156	Orf32-80α -3mB	CGCGGATCCATCGAGTTTAAAGAAGGAGCC
	Orf25phi11-6m	GAAACAGGCAAGATAGCTGCAGGATATCACGGC
	Orf25phi11-7c	GCCGTGATATCCTGCAGCTATCTTGCCTGTTTC
	Orf32-80α-6cS	ACGCGTCGACGCATCATTCTTAACATAGCCC
pJP943	Orf32-80α -3mB	CGCGGATCCATCGAGTTTAAAGAAGGAGCC
	Orf25-phi11-51c	GCCGTGATAACCCGCGTTTATCTTGCC
	Orf32phi80a-50m	GGCAAGATAAACGCGGGTTATCACGGC
	Orf32-80α-6cS	ACGCGTCGACGCATCATTCTTAACATAGCCC
pJP972	Orf32-80α -3mB	CGCGGATCCATCGAGTTTAAAGAAGGAGCC
	Orf25-phi11-57c	CCTAAATTGCCGTGAGCTCCCGCGTC
	Orf25-phi11-56m	GACGCGGGAGCTCACGGCAATTTAGG
	Orf32-80α-6cS	ACGCGTCGACGCATCATTCTTAACATAGCCC
pJP973	Orf32-80α -3mB	CGCGGATCCATCGAGTTTAAAGAAGGAGCC
	Orf25-phi11-53c	GCCGTGAATTCCCGCGTCTATCTTGCC
	Orf25-phi11-52m	GGCAAGATAGACGCGGGAATTCACGGC
	Orf32-80α-6cS	ACGCGTCGACGCATCATTCTTAACATAGCCC
pJP974	Orf32-80α -3mB	CGCGGATCCATCGAGTTTAAAGAAGGAGCC
	Orf25-phi11-55c	GCCGTGAAATCCCGCGTCTATCTTGCC
	Orf25-phi11-54m	GGCAAGATAGACGCGGGATTTCACGGC
	Orf32-80α-6cS	ACGCGTCGACGCATCATTCTTAACATAGCCC
pJP1141	Orf32-80α -48mB	CGCGGATCCGGATGACACAAATGAATAATCG
	Orf25-phi11-63c	AACACTTTCGAACTCCTCCACTTGC
	Orf32-80α -53m	GCAAGTGGAGGAGTTCGAAAGTGTTTAAAGACATATTAGATAGA GTCAAGG
	Orf32-80α-6cS	ACGCGTCGACGCATCATTCTTAACATAGCCC
pJP1136	Orf32-80α -3mB	CGCGGATCCATCGAGTTTAAAGAAGGAGCC
	orf32-phi80a-38m	CTTTTTAAGAAACATATGCAATA
	orf32-phi80a-39c	CAATATTGCATATGTTTCTTAAA
	orf32-phi80a-40m	GGCTTCGGAAGTTGCGGAGTGTAAAGACATATTAGATAG
	orf32-phi80a-41c	CTTTACACTCCGCAACTTCCGAAGCCTTTTTCTCCAC
	Orf32-80α-6cS	ACGCGTCGACGCATCATTCTTAACATAGCCC
pJP980	Orf31phi80α-1mB	CGCGGATCCCGTTAATCTGGAAAGATGGGG
	orf31-phi80alpha-5c	CATCGTGATCTTTATAATCCATTTTCCTATTCCTCCTCATATTTA
	orf32-phi80alpha-29m	ATGGATTATAAAGATCACGATGGCGATTATAAAGATCACGATATC GATTATAAAGATGATGATGATAAAATGACTAACACATTACAAGTAA AA
	Orf31phi80α-4cS	ACGCGTCGACCTGACCCACTTTAATAACTGC

Plasmids	Oligonucleotides	Sequence (5´-3´)
pJP1132	Orf32phi80α -12mB	CGCGGATCCATGACTAACACATTACAAGTAAAAC
pJP1133	Orf32phi80α -13cS	ACGCGTCGACTCTTTACACTCCGCTACTTCC
pJP1143		(these plasmids were constructed using the same oligonucleotides but different DNA templates)
pJP1144		
pJP1145		
pJP1147		
pJP1146	Orf32phi80α -12mB	CGCGGATCCATGACTAACACATTACAAGTAAAAC
	Orf32-80alpha-54cS	ACGCGTCGACTCTTTAAACACTTTCGAACTCCTCC
pJP1147	Orf32phi80α -12mB	CGCGGATCCATGACTAACACATTACAAGTAAAAC
	Orf32-phi80alpha-31cH	CCCAAGCTTCTTGACTCTATCTAATATGTC
pJP1157	Orf32-80α-17m	ATGGATTATAAAGATCACGATGGCGATTATAAAGATCACGATATC GATTATAAAGATGATGATGATAAAATGACTAACACATTACAAGTAA AAC
pJP1158		
pJP985		
pJP982	Orf32-80α-2cB	CGCGGATCCTCACCAAAACCTCCTTGACTC
pJP983	Orf32-80α-18mS	ACGCGTCGACATTATGGCAGGTCAAGTTGTCTATAAATATGAGGA GGAATAGGAAAATGGATTATAAAGATCACGATGG
pJP1159		
pJP1160		(these plasmids were constructed using the same oligonucleotides but different DNA templates)
pJP812	ORF25-phi11-36mS	ACGCGTCGACGAAATTGAGAATAGCGTTTGCTACAGCTAGGGAG GAGCAGGAAAATGGATTATAAAGATCACGATGG
	Orf25-phi11-35m	ATGGATTATAAAGATCACGATGGCGATTATAAAGATCACGATATCG ATTATAAAGATGATGATGATAAAATGACTAACACATTACAAGTAAG G
	ORF25-phi11-5cB	CGCGGATCCCTTGACTCGATCTAAGATGTC
pJP1161	ORF25-phi11-36mS	ACGCGTCGACGAAATTGAGAATAGCGTTTGCTACAGCTAGGGAG GAGCAGGAAA ATGGATTATAAAGATCACGATGG
	Orf25phi11-6m	GAAACAGGCAAGATAGCTGCAGGATATCACGGC
	Orf25phi11-7c	GCCGTGATATCCTGCAGCTATCTTGCCTGTTTC
	ORF25-phi11-5cB	CGCGGATCCCTTGACTCGATCTAAGATGTC
pJP1162	Orf26-phi71-3xflag-1mS	ACGCGTCGACATGAAATTAATGTAGAGGTGGAACAGGAAAATGG ATTATAAAGATCACGATGGC
	Orf26phi71-3xflag-2m	ATGGATTATAAAGATCACGATGGCGATTATAAAGATCACGATATC GATTATAAAGATGATGATGATAAAATGACTAACACATTACAAGTAA AA
	Orf26-phi71-3cB	CGCGGATCCCCCCAAAACCTCCTTGACTCG
pJP1163	Orf26-phi71-3xflag-1mS	ACGCGTCGACATGAAATTAATGTAGAGGTGGAACAGGAAAATGG ATTATAAAGATCACGATGGC
	ORF26-phi71-4m	GAAACAGGCAAGATAGCTGCAGGATATCATGGT
	ORF26-phi71-5c	ACCATGATATCCTGCAGCTATCTTGCCTGTTTC
	Orf26-phi71-3cB	CGCGGATCCCCCCAAAACCTCCTTGACTCG
Probe	**Oligonucleotides**	**Sequence (5´-3´)**
SaPIbov1	SaPIbov1-112mE	CCGGAATTCAATTGCTGAGGCAAAACTTC
	SaPIbov1-113cB	CGCGGATCCTAATTCTCCACGTCTAAAGC

Sequences recognized by the restriction enzymes used in cloning are underlined

References

Arnaud, M., Chastanet, A., and Débarbouillé, M. (2004). New vector for efficient allelic replacement in naturally nontransformable, low-GC-content, gram-positive bacteria. Appl. Environ. Microbiol. *70*, 6887–6891.

Charpentier, E., Anton, A.I., Barry, P., Alfonso, B., Fang, Y., and Novick, R.P. (2004). Novel cassette-based shuttle vector system for gram-positive bacteria. Appl. Environ. Microbiol. *70*, 6076–6085.

Tormo-Más, M.Á., Mir, I., Shrestha, A., Tallent, S.M., Campoy, S., Lasa, Í., Barbé, J., Novick, R.P., Christie, G.E., and Penadés, J.R. (2010). Moonlighting bacteriophage proteins derepress staphylococcal pathogenicity islands. Nature *465*, 779–782.

Úbeda, C., Barry, P., Penadés, J.R., and Novick, R.P. (2007). A pathogenicity island replicon in *Staphylococcus aureus* replicates as an unstable plasmid. Proc. Natl. Acad. Sci. U.S.A. *104*, 14182–14188.